Review

Key Features of TEMPO-Containing Polymers for Energy Storage and Catalytic Systems

Anatoliy A. Vereshchagin [1] [iD], **Arseniy Y. Kalnin** [1,2] [iD], **Alexey I. Volkov** [1], **Daniil A. Lukyanov** [1] and **Oleg V. Levin** [1,2,*] [iD]

1   Institute of Chemistry, Saint Petersburg University, 7/9 Universitetskaya nab., St. Petersburg 199034, Russia; anatoliy_ve@mail.ru (A.A.V.); arseniykalnin@gmail.com (A.Y.K.); grulfex@gmail.com (A.I.V.); lda93@yandex.ru (D.A.L.)
2   Sirius University of Science and Technology, 1 Olympic Ave., Sochi 354340, Russia
*   Correspondence: o.levin@spbu.ru

Abstract: The need for environmentally benign portable energy storage drives research on organic batteries and catalytic systems. These systems are a promising replacement for commonly used energy storage devices that rely on limited resources such as lithium and rare earth metals. The redox-active TEMPO (2,2,6,6-tetramethylpiperidin-1-oxyl-4-yl) fragment is a popular component of organic systems, as its benefits include remarkable electrochemical performance and decent physical properties. TEMPO is also known to be an efficient catalyst for alcohol oxidation, oxygen reduction, and various complex organic reactions. It can be attached to various aliphatic and conductive polymers to form high-loading catalysis systems. The performance and efficiency of TEMPO-containing materials strongly depend on the molecular structure, and thus rational design of such compounds is vital for successful implementation. We discuss synthetic approaches for producing electroactive polymers based on conductive and non-conductive backbones with organic radical substituents, fundamental aspects of electrochemistry of such materials, and their application in energy storage devices, such as batteries, redox-flow cells, and electrocatalytic systems. We compare the performance of the materials with different architectures, providing an overview of diverse charge interactions for hybrid materials, and presenting promising research opportunities for the future of this area.

1. Introduction

At present, inorganic compounds dominate the market of electrode materials for various electrochemical energy storage systems. This raises some issues, especially in lithium-ion batteries that employ nickel- and cobalt-based compounds, which poses problems of price, safety, toxicity, and ethics [1,2]. Hence, the replacement of such materials by environmentally friendly organic compounds is vital for the development of sustainable energy systems. These devices range from supercapacitors and batteries that utilize internal redox transformations of organic materials to fuel cells where the catalytic activity of organic compounds helps produce electrical energy from various fuel species [3]. As a result, fast development of the emerging research topics focused on the creation of novel organic and metal–organic materials with designed functionality produces hundreds of publications both on theoretical and empirical aspects in this area. Attractive candidates for both storage and catalytic applications exist among polymers bearing organic radical substituents as high capacitance groups [4]. One of the most prominent is the group of organic polymers bearing stable nitroxyl radicals, such as 2,2,6,6-tetramethylpiperidine-1-oxyl (TEMPO) [5,6]. The attractiveness of use of such organic radical polymers in batteries

and supercapacitors is due to the high cell voltage and theoretical specific capacitance. At the same time, unpaired electrons of nitroxyl radicals ensure high catalytic activity of such compounds, which is promising for fuel cells and catalytic synthesis. The stability of polymeric materials in target solvents during electrochemical transformations is the most important challenge addressed by the molecular design of nitroxyl radical-containing polymers. To reach the best stability, two separate problems should be solved: chemical stability of the target molecule and solubility of the material in the adjacent electrolyte. Additional requirements may be applied to the materials made for specific applications, such as particular size of the polymer molecules or polymer solution viscosity, crucial for redox-flow cells with porous membranes. Molecules matching these requirements should retain basic features of the materials based on nitroxyl radicals, such as charge–discharge reversibility, energy storage capacity and catalytic activity. Moreover, low electronic conductivity of materials based on nitroxyl radicals limits the rate of charge transfer inside the polymer layer. It hampers broad application of such polymers as an electroactive material both in energy storage and electrocatalysis. Therefore, the design and synthesis of novel materials based on nitroxyl radicals that possess high conductivity while retaining high power density or catalytic activity represents another relevant problem in the development of new polymers. Abovementioned technological challenges inspire numerous publications focused on molecular design, synthetic approaches, and material chemistry of nitroxyl radical-containing polymers. Topical reviews, focused on energy storage [4,5,7–12] or electrocatalytic materials [7,9,13,14], usually pay little attention to systematic study of the features of such polymers. In this context, we prepared the present review of the advances in design and synthesis of novel polymer materials based on nitroxyl radicals, which, we hope, will be useful for researchers focused on the development of new kinds of electrochemical power sources.

2. Electroactive Materials Based on TEMPO

2.1. Synthetic Approaches

Due to continuously growing production, the cost of TEMPO derivatives, and especially 4-hydroxy-TEMPO (TEMPOL) is drastically decreasing. For example, according to the Sigma-Aldrich catalogues, the price of the TEMPOL in 2010 was EUR 295.5 per 25 g of 97% purity substance, while in 2022 the same package costs only EUR 49.9, and the price of the technical grade substance on industrial marketplaces lies below EUR 10/kg. The synthetic route for TEMPO consists of three simple stages, namely condensation of acetone with ammonia, reduction of the carbonyl group and oxidation of the N-H fragment, which makes the TEMPOL an inexpensive building block for industrial production of the functional materials for energy storage and other applications.

TEMPOL itself is an ecological-friendly and non-toxic (LD50 1 g/kg, oral, rat) substance, considered as an antioxidant and drug precursor [15,16]. Unlike many inorganic high-energy materials, TEMPO-based polymers have no tendency of thermal runaway, are non-toxic and non-corrosive and, like most of the polymeric materials, can be disposed of by incineration. Due to these factors, TEMPO provides environmental and operational safety.

2.1.1. Non-Conductive Backbones

Proper selection of the compatible polymeric backbones to bear TEMPO groups is the main step in obtaining the material with the best properties for the desired purpose. Such factors as dissolution of the material, which directly causes device self-discharge [10], and its electrochemical stability, define the choice of backbone polymers [7]. At the same time, due to the complex chemical behavior of nitroxyl compounds, synthetic availability also plays a significant role. Due to this reason, low-cost 4-hydroxy-TEMPO, or TEMPOL, is the most popular precursor for the synthesis of TEMPO-containing monomers by attachment via the hydroxyl group. Alternatively, significantly more expensive 4-carboxy- or 4-amino-derivatives of TEMPO may be used. Although most of the reported syntheses of these

polymers use TEMPO-containing monomers, another option is to introduce TEMPO by the polymer-analogous transformations.

Without any doubt, poly(2,2,6,6-tetramethylpiperidine-*N*-oxyl-4-oxymethacrylate) (PTMA) is the most popular TEMPO-containing polymer for energy storage purposes. Despite the presence of the nitroxide moiety imposing appreciable restrictions on the polymerization techniques, PTMA can be obtained by direct polymerization of 2,2,6, 6-tetramethylpiperidine-*N*-oxyl-4-oxymethacrylate using anionic [17] or group-transfer polymerization [18]. The same synthetic approaches are used to prepare other TEMPO-modified polyalkenes based on acrylamides [19], vinyl ethers [20] or more complicated systems [21]. Another way to introduce nitroxide functionality is by oxidation of the properly functionalized polymers using peroxide oxidants [22] or using starting materials with the reduced TEMPO protected by O-alkylation [23] (Figure 1).
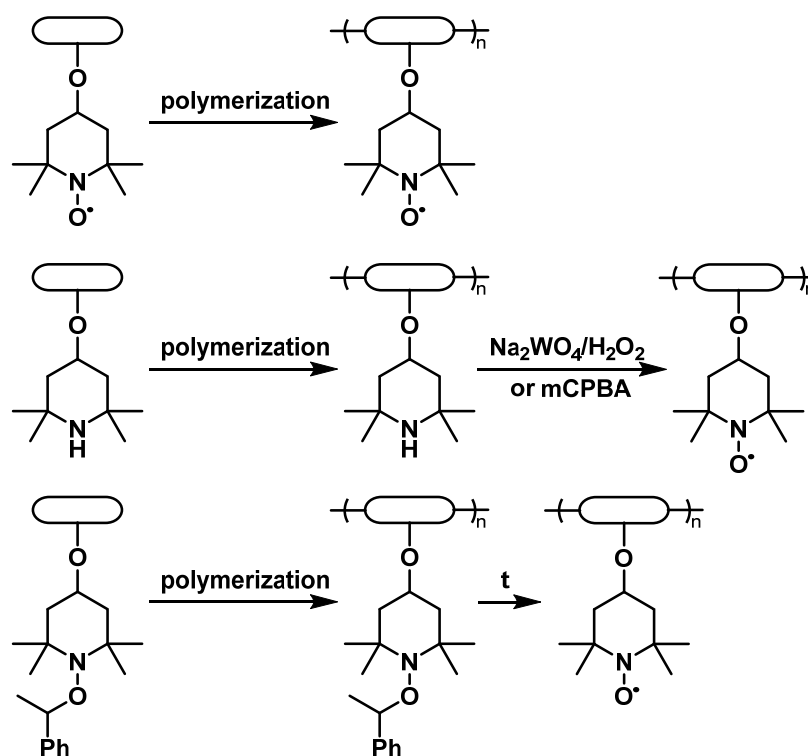
**Figure 1.** Polymerization of unprotected and protected TEMPO-containing monomers.

Other approaches are also useful for the preparation of TEMPO-containing polymers, including ring-opening anionic polymerization of TEMPO glycidyl ether [24], ring-opening metathesis polymerization of TEMPO-containing cyclic alkenes [25], or Michael polyaddition of TEMPOL-acetylacetates to acrylate dendrons [26]. Cross-linked [27], grafted [28], or bifunctional [29] TEMPO-containing polymers are accessible by the copolymerization using the same approaches.

Post-modification of the polymers with the TEMPO-containing blocks is rarely employed, but several examples exist, including the modification of polyimine [30] and poly(ethylene-*alt*-maleic anhydride) [31]. Natural polymers, such as cellulose, can also be employed as carriers of the TEMPO fragments attached by esterification [32].

2.1.2. Conductive Backbones

Most TEMPO-bearing conductive polymers are prepared by electrochemical or chemical oxidative polymerization of TEMPO-containing monomers (Figure 2). Electrochemical polymerization results in deposition of the polymer films directly on the electrode, which is a convenient method for the formation of thin films suitable for electrocatalytic purposes or for basic electrochemical characterization of the materials. At the same time, polymerization

with chemical oxidants allows preparative scale synthesis of the conductive polymer for use in the fabrication of battery cell electrodes. Chemical oxidative polymerization is mostly conducted using $FeCl_3$ in the presence of CH_3NO_2 [33] with ammonium persulfate [34]. Alternatively, Kumada polycoupling of 2,5-dihalothiophene may replace electrochemical polymerization [35].
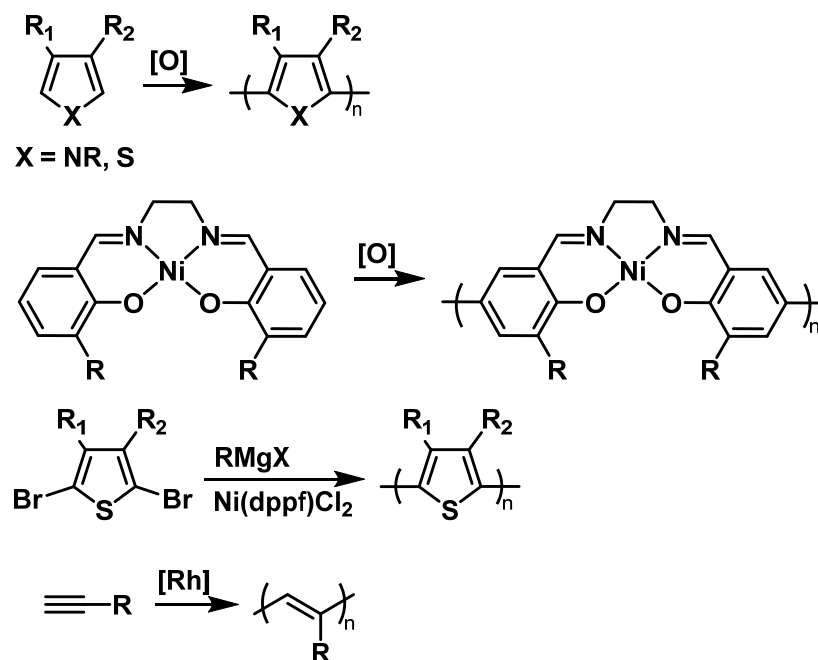
Figure 2. Typical polymerization schemes for the preparation of functional conductive polymers.

Polyacetylenes with TEMPO fragments are not available by oxidative polymerization but can be synthesized by rhodium-catalyzed polymerization of terminal acetylenes [36].

Several classes of electron-reach (hetero)aromatic molecules such as anilines, pyrroles, and thiophenes represent the monomers for the TEMPO-modified conductive polymers. Due to the complex chemical behavior of these fragments, the synthetic approaches to obtain these monomers are often more complicated than the polymerization approaches.

Polymerization of pyrrole proceeds at the 2- and 5-positions, which allows functionalization with TEMPO by *N*-alkylation, followed by attachment of TEMPO to the resulting linker [37,38]. High selectivity of *N*-alkylation makes this approach the most convenient for the synthesis of pyrrole-based monomers. Thiophenes show the same polymerization behavior, but alkylation at the 1-position is unavailable, so the TEMPO fragments are attached to the 3-position of the thiophene ring via ether [39] or ester [33] linker. 2-HydroxymethylEDOT is also used as a precursor for the TEMPO-containing thiophene monomer [40]. Rare examples of the electrochemically polymerizable TEMPO-modified triphenylamine [41] and nickel Salen complex [42] were also reported.

2.2. Fundamental Electrochemistry of TEMPO Transformations

TEMPO is the founding piece among organic radicals for energy storage applications, as well as a touchstone for other similar materials. Its use for lithium-ion batteries can be traced back to 2002 [43], when Nakahara et al. employed a TEMPO-bearing poly(methacrylate) (PTMA) as an electrode material. Since then, a multitude of polymer backbones has been used in combination with TEMPO and other stable organic radicals [44], as such materials are quite promising. Their main advantages include high stability in standard lithium-ion electrolytes (recharging with negligible loss up to 2000 cycles [31]), and fast recharging time (available current rates of up to 100 C [45]), which results in impressive power density [11,12].

The nitroxide radical can either reversibly oxidize to form an oxoammonium cation (p-doping) or reduce to an aminoxyl anion (n-doping), which is the basis of electrochemical transformations in such materials (Figure 3). These reactions are useful in a variety of applications, allowing the use of TEMPO-based materials in metal-ion batteries, redox flow cells and oxidation catalysts [9,11]. Most reports deal with the oxidation into oxoammonium cation, as this reaction proved to be optimal in terms of its relatively high potential, which is 3.5 V vs. Li/Li$^+$. TEMPO-modified poly(methacrylate) has become a de facto standard material [10] for organic cathodes in lithium-ion cells, which theoretical capacity of 111 mAh g^{-1} can be achieved in practice. There are other options, such as poly(vinyl ether) with 131 mAh g^{-1} [46], and numerous attempts exist to increase this value up to 224 mAh g^{-1} [47]. However, current materials require binders and conductive agents, practically rendering this value unattainable. Utilization of intrinsically conductive polymers as a backbone might improve the situation. There are also options that allow increase in the cell density via shifting the potential of the reaction up to 3.7 V [48].
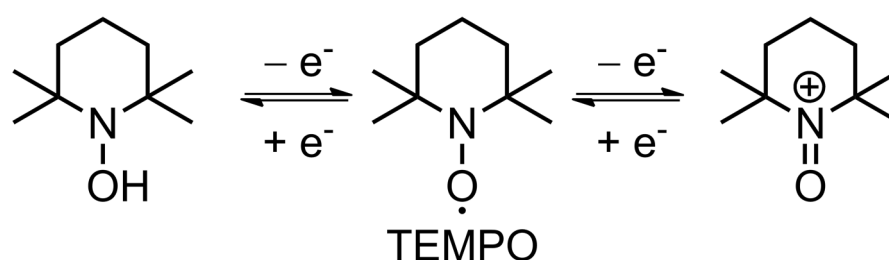
Figure 3. Schematic representation of redox couples of TEMPO radicals.

Regardless, with the average voltage vs. Li being 3.5 V, long cycle life (up to 2000 cycles [31]) and high (up to 100 C [45]) rate capability, TEMPO is an ideal candidate for use in organic radical batteries, with power density rivaling that of standard inorganic materials.

As TEMPO is overwhelmingly used as a pendant group on a polymer backbone, it is reasonable to discuss its electron transfer and doping processes in this context of the whole material, rather than individual TEMPO units. As shown in several studies [49,50], electron transfer mechanism includes two distinct steps. The first one is electron transfer between the substrate and the radical components—a heterogeneous step—and the second is self-exchange between the neighboring radicals, primarily driven by concentration gradients of the moieties (Figure 4). The latter is a homogeneous step and referred to as hopping.
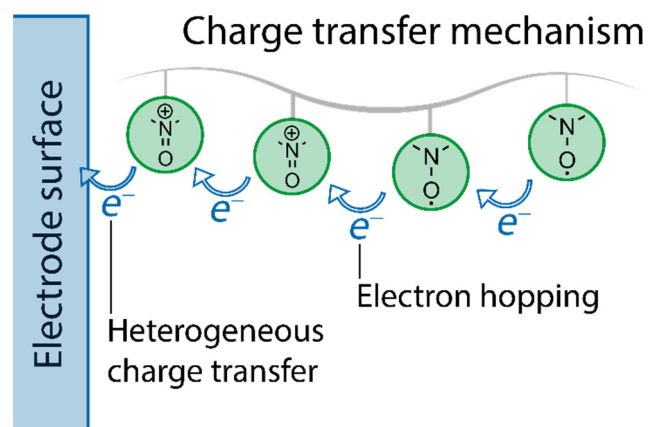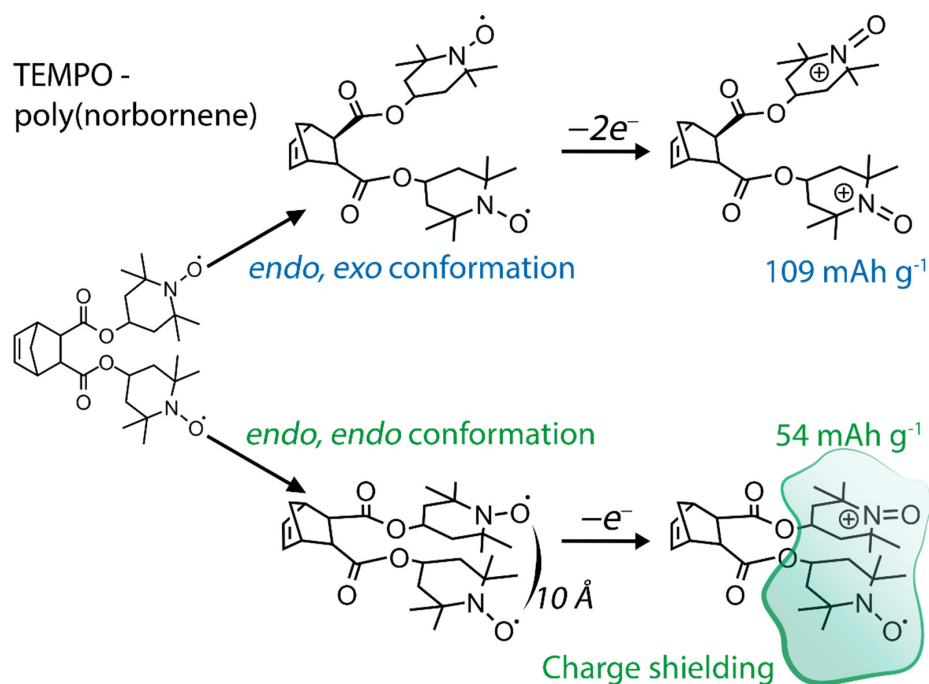

Figure 4. Schematic illustration of the redox reaction in TEMPO-containing polymer between nitroxide radical and oxoammonium cation.

The rate constant of the heterogeneous charge transport is ca. 10^{-1} cm s^{-1} both for TEMPO monomers [51], and for TEMPO in PTMA deposited on Pt surface [52]. The self-exchange between neighboring radicals responsible for the homogeneous transport has

a bimolecular rate constant of 1.8×10^5 M^{-1} s^{-1} [50]. This value is up to four orders of magnitude higher for nitroxide-containing monomers [51,53,54], indicating that attachment of the molecule to the polymer chain hinders diffusion. Still, the fast kinetics cause a small gap between charge and discharge voltages, typically, ca. 100 mV, and allow extraction of almost full capacity of the material at a relatively high 1 C discharge rate: 110 mAh g^{-1} actual capacity vs. 111 mAh g^{-1} theoretical one [22].

For the polymer with 100% of monomer units modified by TEMPO (i.e., PTMA), little to no conformational changes accompany electron transfer. This enables Nernstian adsorbate-like behavior in polymer layers with thickness from 10 nm to 100 nm, which allows the use of thicker films and increase in the content of the polymer in the electrode material [50]. Conversely, the polymer with low density of TEMPO radicals becomes twice as stiff upon oxidation, compared to its reduced state [55]. While the electrochemical processes affect the conformation of the polymer, the monomer structure exerts a significant effect on the performance of the materials, such as their capacity. For example, another popular polymer backbone, poly(norbornene), can be functionalized by two TEMPO moieties per monomer unit. In the case of endo/endo configuration of the modified polymer, the capacity of the material is only 54 mAh g^{-1}, while endo/exo configuration yields full capacity of 109 mAh g^{-1} [56]. Due to the proximity of neighboring TEMPO substituents, which in the endo/endo case are only 10 Å close, the generated positive charge on the first radical prevents oxidation of the second one (Figure 5). This presents the general issue for implementation of organic radical materials with densely packed redox-active groups.

Figure 5. Schematic illustration of influence of neighboring TEMPO groups on molecule oxidation.

Another aspect worth considering is the intramolecular interactions for TEMPO substituents in long polymer chains, which require increased local concentration of charge carriers to make electron hopping more probable [57]. One such option is annealing of a polymer with a TEMPO substituent, which results in formation of percolating networks, increasing the conductivity of the polymer to 10 S m^{-1}, compared to the 1×10^{-9} S m^{-1} of the initial disordered polymer with randomly oriented radical groups [58].

High electron exchange rates notwithstanding, decent electrode materials performance also involves facile ionic transport. This is directly related to the following requirements to the electrode–electrolyte interactions: the polymer should swell, yet be insoluble, to

prevent self-discharging of the electrode [59], and the polymer should be either solvophilic or well-solvated to provide the mobility of the counterions.

The dissolution of the polymer may result in, e.g., 38% self-discharge in one week [22], yet this might be easily prevented by crosslinking [18] of the polymers.

Ensuring ionic conductivity requires tight control over both radical polymer and electrolyte properties. There are multiple factors at play here [4,44,59]. The effect of the porosity of the material matters most in the case of thin-film electrodes, where the increase in thickness would hinder diffusion through the material, as bulk transport becomes the limiting factor [60], which is observed already from the film thickness of 0.26 μm [61]. The pores design may be improved via porous carbon architectures [62], inclusion of porous polymers [63], or development of three-dimensional electrode structures [64].

To ensure electroneutrality, the process of electrochemical oxidation of NO● to N$^+$=O must be accompanied either by anion uptake or by cation expulsion, with the opposite process on reduction. This means that proper selection of material and electrolyte compositions should provide the conditions for high diffusion rates of charged species. Even for typical lithium-ion electrolyte, LiPF$_6$ (in propylene carbonate, PC), the ratio between the number of TEMPO groups in PTMA and LiPF$_6$ molecules strongly affects the performance of the material: changing the LiPF$_6$-to-TEMPO ratio from 1.7 to 0.5 the self-exchange rate constant increases from 0.16×10^6 M^{-1} s^{-1} to 2.8×10^6 M^{-1} s^{-1} [65]. The decrease in the rate constant in highly concentrated electrolyte has to do with decreased mobility of ions—and predominantly with the nature of anions [66–68]—in swollen polymers. It is worth noting, however, that cations also affect the performance of organic radical polymers, e.g., PTMA, and even participate in charge compensation, as shown by electrochemical quartz crystal microbalance [69].

The replacement of the backbone polymer altogether may enhance ionic conductivity. For instance, (poly(2,2,6,6-tetramethylpiperidinyl-*N*-oxyl vinyl ether)) PTVE is hydrophilic, thus providing high affinity to aqueous electrolytes, and ensuring facile ion transport [70]. Another example is (poly(2,2,6,6-tetramethylpiperidinyl-*N*-oxyl glycidyl ether)) PTGE, which has good swelling and ionic transport in standard 1.0 M LiPF$_6$ in ethylene carbonate: diethyl carbonate (EC:DEC) electrolyte, providing up to 80 mAh g^{-1} capacity at 10 C [27].

As a side note, interactions of TEMPO within the battery may bear disruptive effects on other components by virtue of strong oxidizing capability of TEMPO cation. For example, cellulose-based separators are likely to decompose in its presence [71]. This presents an additional challenge when selecting optimal components.

Another way to improve the transport properties is to provide doping mechanisms via backbone polymer itself. This can be achieved by using conjugated polymers [72,73], though the competing redox processes in radical and backbone components complicate the studies of the charge transport mechanism. Still, there is some understanding of such processes. For example, in TEMPO-modified polypyrrole (with acetylene black as conductive component) [37] the charge transfer process is separated in four steps: (1) self-exchange between nitroxide radicals, (2) electron transfer from the radical to the conductive backbone, (3) electric conduction from polypyrrole to acetylene black, (4) electron transfer from acetylene black to the current collector (Figure 6).

Polypyrrole is deemed to be an electric conduction path that assists repeatable oxidation/reduction through aggregated radical polymer bulks. The internal charge transfer between the TEMPO pendant groups and the backbone has also been observed in the case of TEMPO-modified 3,4-propylenedioxythiophene (ProDOT) [74], though the precise effect of such interaction was not firmly established.
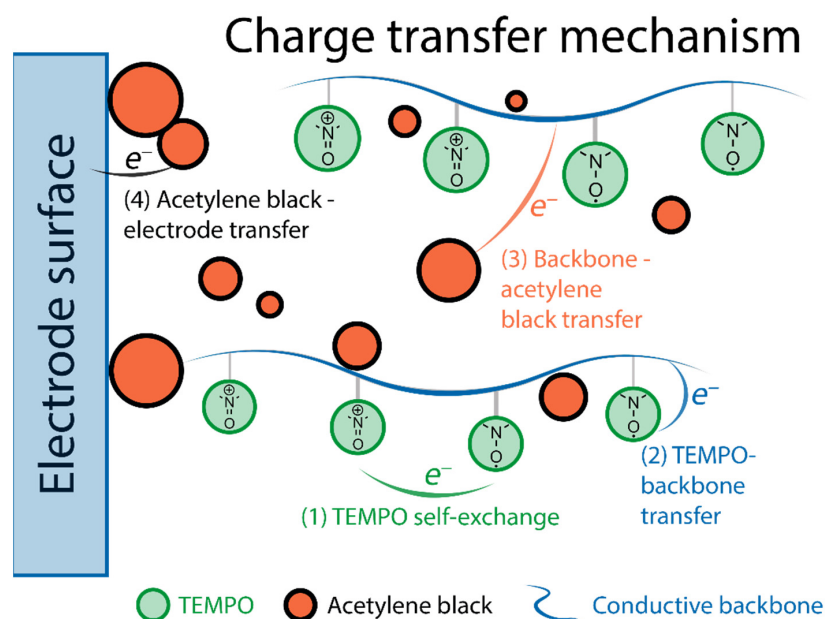
Figure 6. Schematic illustration of the charge transfer process in TEMPO-modified polypyrrole.

Adverse effects of TEMPO radicals have also been reported. In the case of TEMPO-modified poly(3-hexylthiophene) (P3HT) [35], it turns out that intrinsic conductivity of P3HT—controlled both by intrachain and interchain hopping—is hindered by introduction of TEMPO. The impairing effect of TEMPO is due to introduced disorder in crystalline domains of the polymer, which restricts interchain hopping, thus terminating additional paths of charge transfer and decreasing conductivity. The effects of TEMPO content in P3HT on capacity were also investigated [48], and, similarly, the capacity was the highest with the minimal content of TEMPO, while 100% TEMPO-loaded conjugated polymer provided both the lowest specific capacity and the highest charge transfer resistance. Another effect was observed for polythiophenes bearing pendant TEMPO groups [39], where internal transfer of an electron from TEMPO to the polythiophene backbone caused rapid dedoping of the latter. This phenomenon led to a decrease in both capacity and conductivity and due to the thermodynamically favorable conditions: the 3.88 V oxidation potential of polythiophene is higher than that of nitroxide radical (3.60 V), thus facilitating backbone reduction. A reverse scenario, albeit with similar negative effects, was observed for poly(TEMPO−DTP) (TEMPO-modified (dithieno[3,2-b:2′,3′-d]pyrrole)) [75]: the low oxidation potential of poly(DTP) (3.15 V) caused electron transfer from the backbone to the radical upon charging, thus reducing the activity of the polymer and decreasing Coulombic efficiency. This means that the balance must be found in the thermodynamic preference of the reactions, so that the potentials of both charge carriers overlap in such systems.

The discussed mechanisms of electron transport between TEMPO moieties, the employed backbone, their doping, and diffusion of ions, as well as other aspects of intramolecular, intermolecular, and electrode–electrolyte interactions call for rational approach in finding the optimal systems for the highest efficiency and capacity.

3. Application of TEMPO-Containing Polymers in Energy Storage Devices

3.1. Batteries

Low molecular weight of TEMPO-containing monomer fragments, fast charge transport within polymers, and tunable structure of backbones make TEMPO-based organic radical batteries promising energy storage devices (Figure 7). With an average voltage of 3.6 V, capacities of more than 100 mAh g^{-1} and high-rate capability (up to 100 C), the properties of TEMPO-containing batteries compete with those of conventional inorganic batteries. However, many challenges remain to extracting the best properties of the materials, which is linked both to the structure of the polymers, electrode compositions,

electrode–electrolyte interactions, electronic charge transfer and ionic doping mechanisms, etc. Furthermore, we discuss two major subgroups of TEMPO-containing polymers and present the latest trends and developments, as well as the prospects and challenges in this area.
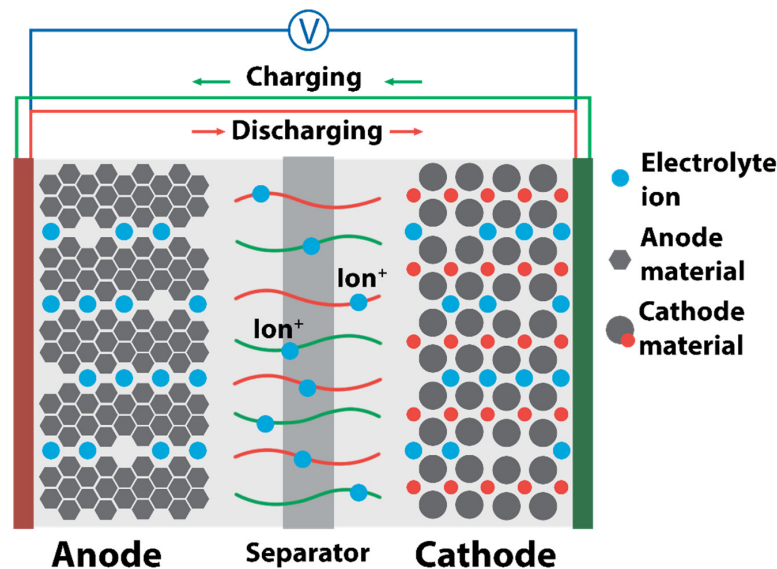

Figure 7. Schematic illustration of organic polymer-based battery.

3.1.1. Radical Polymers

TEMPO-containing polymer materials for batteries are typically created using a grafting approach in which TEMPO groups are attached to the monomer via linkers. The literature describes multiple synthetic approaches utilizing different linkers and backbones. Thanks to such chemical diversity, it is possible to obtain materials that differ significantly in polymer chain length, ionic conductivity, capacity, morphology, etc (Table 1).

Starting with a polymer with the lowest molecular weight of the monomer unit, PTVE, materials **1** and **2** presented by Nakahara and coworkers [20,76] are organic cathode materials with different ratios of vapor-grown carbon fiber (VGCF). The materials showed high performance (104 mAh g^{-1}, which is 77% of PTVE theoretical capacity of 135 mAh g^{-1}) even with an active material content of 80%. Polymer **1** retained up to 32% of initial capacity at high discharge current of 80 C. Due to high solubility in common carbonate-based solvents, PTVE-based cathode materials are rarely found in the studies with typical lithium-ion electrolytes. Nishide et al. [46,70] evaluated the performance of the same polymers **3** and **4** in aqueous zinc-ion batteries where PTVE is insoluble. Along with the high capacity at 60 C (~100% of the theoretical capacity of 131 mAh g^{-1}), the materials show good stability, retaining 75% of the initial capacity after 1000 cycles. In paper [77], Nakahara and coworkers introduced an ethylene oxide chain into the PTVE structure to achieve higher rate capability and power density. Charge/discharge properties of copolymerized PTVE **5** and **6** improved with the length of the ethylene oxide chain. High rate and power properties of the PTVE copolymer were better than those of the PTVE homopolymer. As authors explained, these results indicate that the tri(ethylene oxide) chain of **6**, which has high flexibility, high ionic conductivity, and low steric hindrance, provided PTVE with smooth ionic transport, which leads to improved battery performance.

The most popular organic radical polymer is a TEMPO-grafted polymethacrylate, PTMA. Its ubiquity is due to easy synthesis and availability of creating crosslinked systems. PTMA-based cathodes considered in this review (**7**–**36**) have a capacity of around 75–110 mAh g^{-1} related to TEMPO/TEMPO$^+$ process. The stability of TEMPO radical, lower solubility of polymethacrylate backbone and its amorphous structure provide high cycle-life performance, good capacity and high-rate charge and discharge processes to

PTMA. PTMA also tends to partially dissolve in commonly used carbonate electrolyte solvents where the polymer is solvophilic if its molecular weight is not high enough, affecting the energy density, self-discharge, and cycle life performance of batteries. For this reason, various research groups resort to the synthesis of crosslinked systems, the use of a grafting approach with graphene-like materials, or the fabrication of composites with high loading of binder and conductive agents. A stable reversible redox process involving a TEMPO/TEMPO$^+$ pair is the prevailing one in PTMA-related works, providing maximum theoretical capacity of 111 mAh g^{-1}. Materials **11**–**13** and **35** are systems with two-electron redox processes where the second process is reversible reduction of nitroxide radical to hydroxylamine anion, providing 60–70% of the presented material capacity (221–250 mAh g^{-1}). However, the anions formed in this process are highly soluble, and the redox reaction has a capacitor-like electrochemical response, which makes its use difficult in batteries. Material **36** is an example of a PTMA composite based on polymer complexes of nickel with Schiff bases. This conductive polymer binder has its own redox capacity, allowing creation of a cathodic material without the use of conductive additives. Material **36** reached a capacity of 83 mAh g^{-1} with 55% of the initial value was retained after 1000 cycles.

Materials **37**–**38** are examples of crosslinked systems that require less binder and conductive agents. In the case of **37**, this approach made it possible to achieve high stability (95% of the initial capacity remained after 500 cycles) and relatively high capacity, as compared to other organic materials (73 mAh g^{-1}). System **38** based on crosslinked poly(b-ketoester) networks allowed loading of a high content of active material without additional components. However, the increased mass of the molecule reduces the capacity (55 mAh g^{-1}). The paper [31] presented a solvent-resistant radical polymer bearing multipendant groups (poly(ethylenealt-TEMPO maleate) (PETM) **39**. As dissolution is a detrimental process that causes deterioration of the electrode properties, in this case low solubility of the material bore a positive effect on the cyclic stability (83% of the initial capacity is retained after 2000 cycles). The capacity of the material was close to the theoretical one (90 mAh g^{-1} vs. 119 mAh g^{-1}); however, high content of conductive additives (80% carbon black) did not allow reaching a high capacity of the fabricated cathode. The paper [78] presented material **40** with different contents of pyrene molecules as side groups. The authors achieved close contact between carbon nanotubes (CNTs) and PTMA chains in the composite without the modification of the CNT network, thus not affecting its conductivity. A single terminal pyrene as chain-end unit promoted the immobilization of PTMA chains on the CNT, while a multi-pyrene structure provided interaction of the whole PTMA chain with the CNT. At C/6, cathode **40** delivered a high capacity of 110 mAh g^{-1} (82 mAh g^{-1} at 1 C and 55 mAh g^{-1} at 20 C) and had good cycling stability (87% of initial capacity remained after 170 cycles). Paper [45] presented a method to graft the PTMA as a thick functional layer on an ITO/glass plate by designing glycidyl methacrylate as an anchoring and a frame-forming block segment. The resulting materials **41** and **42** that differ in the content of active material—100% for **41**, and 30% for **42**—have impressive stability and good capacity (for **41** and **42**, 70 mAh g^{-1} at 100 C and 104 mAh g^{-1} at 0.1 C, respectively). Materials **43** and **44** are zwitterionic radical polymers created to reach high density of the Li$^+$ ion incorporation per repeating unit at a positive redox potential. Copolymerization caused efficient self-charge compensation. Unfortunately, the specific capacity of **43** was relatively low (only 20 mAh g^{-1} at 5 C) [67]. Since the molecular weight of **44** is lower, the specific capacity reached 39 mAh g^{-1} even at 10 C due to fast ion transport [79]. To create the material with good solubility during the processing and good solvent resistance during recharging, a new photo-crosslinkable branched nitroxide polymer **45** was synthesized via reversible addition-fragmentation chain-transfer copolymerization of PTMA, cinnamoyl ethyl methacrylate, and ethylene glycol dimethacrylate [80]. Dissolution of as-synthesized polymer in ethyl alcohol, followed by deposition on a substrate and UV-irradiation, produces a crosslinked polymer with low solubility in organic electrolytes. The material **45** had remarkable cycling stability with a capacity retention of 90% over 1000 charge–discharge

cycles at 10 C. On the other hand, the molecular load with only one redox active moiety per three blocks decreased specific capacity, and **45** reached only 65 mAh g^{-1} even with 80% of carbon additives. Another "grafting-through" strategy using anionic polymerization and ring-opening metathesis polymerization was selected to synthesize the TEMPO-crowded bottlebrush polymers [28]. This approach provided easy access to the radical bottlebrush polymers with the well-defined sizes, which were tunable by both side chain and main chain lengths. Due to this molecular tuning, the polymer **46** demonstrated good cyclability (90% of initial capacity retained after 100 cycles) and reached a high capacity of 103 mAh g^{-1} without any additives. The polyallene with stable pendant TEMPO groups **47** showed excellent coulombic efficiency and stability (~98% remains after 50 cycles) but reached only ~34% of the theoretical capacity (40.8 mAh g^{-1}) even with 80% of carbon additives [81].

The materials **48–52** based on poly(TEMPO-substituted glycidyl ether) (PTGE) have a flexible and ionophoric backbone which allows the propagation of charge deep into the polymer layer from the polymer/electrode interface. This reduces the number of conductive components compared to PTMA. The materials show moderate capacities of 59–80 mAh g^{-1}, and crosslinked materials **48** and **51** also demonstrated remarkable cycling stability (~99% remained even after 1000 cycles). Poly(TEMPO-substituted ethylene sulfide) **53** yielded ionic conductivity approximately three times higher than that of the corresponding polyether [82]. The material showed high capacity (83 mAh g^{-1}) even with 95% content of active material, which indicates strong influence of the molecule structure on the polymer electrochemical properties.

The next group of materials is the family of polyacrylamide-based structures—PTAm **54–58**. They are water-insoluble, but sufficiently water-swellable electrode-active polymers, and thus are commonly applicable in aqueous electrolytes. Materials **54–58** reached capacities of 60–114 mAh g^{-1}, which is a good result for organic materials. The material **55** showed the highest stability in water-based electrolyte (80% of the initial capacity remains after 2000 cycles) [19]. Modification of PTAm **56** with sodium styrene sulfonate produced a hydrophilic radical polymer **58** [29]. This allowed the polymer **58** to adapt to a wider range of electrolyte solutions and significantly increased its cycling stability in an organic-solvent-based electrolyte (95% vs. 63% of initial capacity retained after 100 cycles for **58** and **56** materials, respectively).

Materials **59–62** are based on a poly-norbornene backbone. Poly-norbornene provides good film formability, compatibility with the current collectors, and contains prospective sites for photocrosslinking after molding. Such materials showed high capacities (70–100 mAh g^{-1}), and low solubility allowed the use of **59–62** in carbonate solvents with high stability. Poly(7-oxanorbornenes) can exist in a variety of microstructures capable of interaction with cations via oxygen in the polymer backbone. Materials **63** and **64** were created [25] to determine whether the poly(7-oxanorbornene) skeleton provides an advantage over the polynorbornene backbone in polymers with pendant TEMPO side chains. The capacity of the **63** and **64** reached 107 mAh g^{-1} and 92.8 mAh g^{-1}, respectively, corresponding to 98.3% and 85% of their theoretical capacity value. In the case of **64**, the capacity increased during the cycling stability test, which appears to arise from the increase in the contact surface between the electrode and the electrolyte due to the swelling of the polymer during the test.

Materials **65** and **66** are the small molecular nitroxide radicals consisting of triazole rings with theoretical capacities of 111–131 mAh g^{-1} [83]. The negligible solubility and compact crystal structure of **66** enabled better interaction and dispersion in the carbon matrix and the binder, thereby facilitating overall better cell performance than **65**. It also allowed a high mass percentage in the electrode composition (up to 80 wt%) without compromising the electrochemical performance. Both materials demonstrated high capacity and remarkable stability with retention of initial capacity of up to 96% after 200 cycles.

A low-temperature, efficient, and simple synthetic strategy allows attainment of the polystyrene-based compound **67** [21]. Unfortunately, the material demonstrated poor

capacity properties (31 mAh g^{-1}). Authors explained that several factors may have resulted in low capacity, including electrostatic effects (reduction in the possibility of positive charge forming on the adjacent TEMPO units upon oxidation), limited counter ion diffusion into the bulk of the composite material (required to compensate for the positive charge forming upon oxidation), insufficient rate of redox reaction, and limited rate of electron transport within the polymeric material induced by large separation between TEMPO units. On the other hand, **67** demonstrated stable work during 80 charge/discharge cycles which indicates low solubility in carbonate electrolytes.

The synthesis of novel polymer ionic liquids based on polyvinylimidazolium bearing a pendant nitroxide radical on each monomer unit **68** aimed at prevention of the dissolution and/or diffusion of the redox-active group in the electrolyte and thus improvement of the cycling performance and rate capability of batteries [23]. Material **68** was coated onto buckypaper and tested as a cathode in a lithium-ion battery. Material **68** demonstrated remarkable initial capacity (170 mAh g^{-1} at 1 C) which decreased to 78 mAh g^{-1} and stabilized after 100 cycles. An outstanding achievement is that 100% of the initial capacity remains even after 1300 cycles at 60 C. A similar material **69** partially functionalized with triethylene oxide was presented in [84]. By combining the redox activity of TEMPO and remarkable ionic conductivity of poly(trimethylene oxide) blocks, outstanding rate capability performance was achieved with a remarkable capacity of 69 mAh g^{-1} even at 60 C. This result is higher than that of material **68**. Material **69** also demonstrated higher stability, preserving 92% of the initial discharge capacity after 3600 cycles. Other two types of ionic liquid-supported TEMPO radical and imidazolium hexafluorophosphate were synthesized [85,86]. The mono-(**70**) and di-radicals (**71**, **72**) with theoretical capacities of 59 mAh g^{-1} and 80 mAh g^{-1}, respectively, can be used as materials for the room temperature operation of the battery, exhibiting high-rate capability and stable cycling properties. Material **70** reached 59 mAh g^{-1}, and **71**, **72**, with higher content of TEMPO, reached 80 mAh g^{-1}. All materials showed good cyclability, and **71**, **72** saved up to 99% of the initial capacity after 50 cycles.

Polysiloxane was used as a backbone for TEMPO substituents to create more eco-friendly and cheap cathodes [87]. Materials **73** and **74** were fabricated with the addition of vapor-grown carbon fiber. Material **73** showed the discharge capacity of 46 mAh g^{-1}, which is 47% of its theoretical capacity (98 mAh g^{-1}). This result is low because of the lower radical concentration in the total mass of the polymer. To minimize the monomer mass, **74** was created. The theoretical capacity of **74** (116 mAh g^{-1}) is larger than that of not only silicone-based polymer **73** but also PTMA (111 mAh g^{-1}). Material **74** reached 89 mAh g^{-1} and demonstrated stable work during 100 cycles in a carbonate-based electrolyte.

Materials **75**–**80** were obtained by grafting approach using high-surface-area substrate as a carrier, e.g., cellulose or graphene, and conductivity is an additional benefit of the latter.

Materials **78** and **79** were used as high-capacitance intercalation anode materials. The complication of the carrier structure from **75** to **80** allows the materials to achieve higher values of capacity and stability. Material **80** formed on the multiradical-stabilized hollow carbon spheres matrix reached capacities of 330 mAh g^{-1}. About half of it is related to the TEMPO/TEMPO$^+$ redox process. It has been shown that the material can work in organic solvents with Li$^+$ or Na$^+$ electrolytes with good stability (82% of initial capacity remained after 200 cycles) [88].

Alternative material structures include star polymers characterized by decreased chain entanglement compared to the linear structures, which may enhance the diffusion of counter ions. Material **81** was synthesized based on a triphenylamine core [89]. This configuration allowed a two-electron redox process related to TEMPO recharging, yet it did not result in high capacity. Phosphazene core-based **82** had a lighter molecule compared to **81** [90]. A two-electron redox process also occurred in material **82**, thus reaching a capacity of 115 mAh g^{-1}, which emphasizes the importance of selecting the molecular structure of the material.

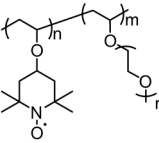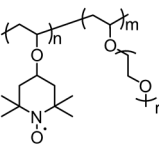Table 1. Structures and energy storage performance of the TEMPO-containing polymers with non-conductive backbones.

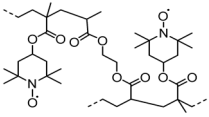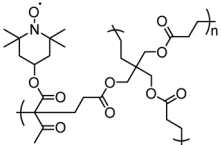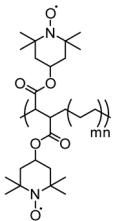| No.	Material Structure	Electrode Composition (Active:Conductive:Binder) / %	Negative Electrode	Electrolyte	Output Voltage vs. Li$^+$ / V	Capacity Retention / % of Initial Capacity	Current / C	Capacity per Electrode Mass (Polymer mass) / mAh g^{-1}	Ref
1		80:15:5	Li	1 M LiPF$_6$ / EC:DEC	3.5	n/a	1	83(104)	[76]
2		20:70:10	Li	1 M LiPF$_6$ / EC:DEC	3.5	n/a	0.6	23(114)	[20]
3		100:0:0	Zn	0.1 M NH$_4$Cl / H$_2$O	1.7 vs. Zn/Zn^{2+}	75 after 1000 cycles	60	131(131)	[70]
4		100:0:0	Zn	0.1 M NaCl / H$_2$O	0.75 vs. Ag/AgCl	75 after 1000 cycles	60	131(131)	[46]
5		10:60:30	Li	1 M LiBETI / EC:DEC	3.55	n/a	1	10(103) r = 1	[77]
6		10:60:30	Li	1 M LiBETI / EC:DEC	3.55	n/a	1	11(113) r = 3	[77]
7		25:75:10	Li	1 M LiClO$_4$ / EC:DEC	3.6	96 after 370 cycles	10	23(94)	[91]
8		100:0:0	Pt	0.1 M TBAClO$_4$ / AN	0.4 vs. Ag/AgNO$_3$	90 after 50 cycles	10	97(97)	[92]
9		100:0:0	Li	0.1 M LiTFSI / EC:DEC	3.65	97 after 100 cycles	20	94(94)	[93]
10		30:60:10	Li	1 M LiPF$_6$ / EC:DMC	3.6	80 after 500 cycles	1	40(133)	[94]
11		100:0:0	Li	1 M LiPF$_6$ / EC:DMC	3.6/2.9	88 after 100 cycles	0.1	221(221)	[95]
12		10:80:10	Li	1 M LiPF$_6$ / EC:DMC:DEC	3.6/2.9	45 after 20,000 cycles	1	22(222)	[96]

Table 1. *Cont.*

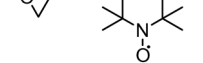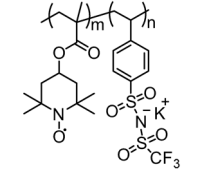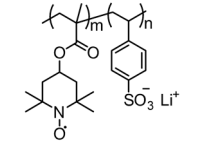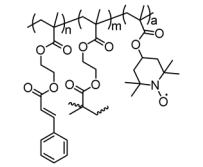| No.	Material Structure	Electrode Composition (Active:Conductive:Binder) / %	Negative Electrode	Electrolyte	Output Voltage vs. Li$^+$ / V	Capacity Retention / % of Initial Capacity	Current / C	Capacity per Electrode Mass (Polymer mass) / mAh g^{-1}	Ref
13		80:10:10	Li	1 M LiPF$_6$ / EC:DMC	3.6	77 after 300 cycles	1	182(228)	[96]
14		100:0:0	Li	1 M LiPF$_6$ / EC:DMC:DEC	3.65	87 after 200 cycles	0.5	94(94)	[97]
15		100:0:0	Li	1 M LiPF$_6$ / EC:DEC	3.6	72 after 150 cycles	0.5	111(111)	[98]
16		30:60:10	Li	1 M LiPF$_6$ / EC:PC:DEC	3.6	88 after 100 cycles	1	27(90)	[99]
17		90:10:0	Li	1 M LiPF$_6$ / EC:PC:DEC	3.6	85 after 1200 cycles	10	49(55)	[100]
18		80:20:0	Li	1 M LiTFSI / EC:DEC:DMC	3.7	70 after 80 cycles	1	12(15)	[101]
19		56:29:10	Li	1 M LiPF$_6$ / EC:DEC	3.6	96 after 1000 cycles	1	61(103)	[17]
20		60:30:10	Li	1 M LiPF$_6$ / EC:DMC	3.6	99 after 10 cycles	50	65(109)	[102]
21		40:50:10	Li	1 M LiPF$_6$ / EC:DMC	3.6	90 after 100 cycles	1	44(111)	[103]
22		60:30:10	Li	1 M LiPF$_6$ / EC:DMC	3.6	88 after 200 cycles	1	47(79)	[104]
23		80:10:10	Li	1 M LiPF$_6$ / EC:DMC	3.6	90 after 50 cycles	1	88(110)	[105]
24		50:30:20	Li	1 M LiPF$_6$ / EC:DMC	3.6	91 after 150 cycles	10	56(111)	[106]
25		25:65:10	Li	1 M LiPF$_6$ / DMC	3.6	99 after 300 cycles	1	17(67)	[107]
26		40:50:10	Li	1 M LiPF$_6$ / EC:DMC	3.6	84 after 100 cycles	30	44(111)	[108]
27		10:80:10	Pt	0.1 M TBABF$_4$ / AN	3.6	99 after 1000 cycles	10	8(77)	[109]
28		50:45:5	Graphite	1 M LiPF$_6$ / EC:DEC	3.5	82 after 100 cycles	1	40(80)	[110]

Table 1. *Cont.*

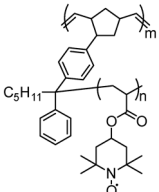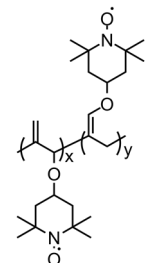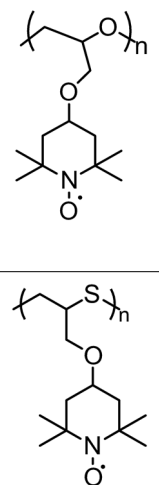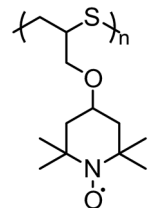| No.	Material Structure	Electrode Composition (Active:Conductive:Binder) / %	Negative Electrode	Electrolyte	Output Voltage vs. Li$^+$ / V	Capacity Retention / % of Initial Capacity	Current / C	Capacity per Electrode Mass (Polymer mass) / mAh g^{-1}	Ref
29		50:45:5	Li	1 M LiPF$_6$ / EC:DEC	3.6	92 after 100 cycles	1	55(110)	[22]
30		60:35:5	Carbon	1 M Pyr14TFSI / PC	0.7 vs. Ag/Ag$^+$	n/a	0.2	58(96)	[111]
31		77:15:8	Li	1 M LiPF$_6$ / EC:DMC	3.6	98 after 100 cycles	1	60(78)	[112]
32		10:80:10	Li	1 M LiPF$_6$ / EC:DEC	3.5	88 after 500 cycles	0.1	8(77)	[43]
33		40:50:10	Li	1 M LiPF$_6$ / EC:DMC	3.6	85 after 400 cycles	10	44(110)	[113]
34		27:46:27	Li	1 M LiPF$_6$ / EC:DMC	3.6	95 after 200 cycles	2	26(97)	[18]
35		50:50:0	Li	1 M LiPF$_6$ / DMC	3.6	82 after 100 cycles	1	125(250)	[114]
36		100:0:0	Carbon	1 M LiClO$_4$ / H$_2$O	0.6 vs. Ag/AgCl	55 after 1000 cycles	1	83(83)	[115]
37		70:21:9	Li	1 M LiPF$_6$ / EC:DMC	3.6	95 after 500 cycles	1	73(104)	[116]
38		100:0:0	Pt	0.5 M (n-C$_4$H$_9$)$_4$NClO$_4$ / AN	0.8 vs. Ag/AgCl	n/a	1	55(55)	[26]
39		10:80:10	Li	1 M LiPF$_6$ / EC:DEC:EMC	3.6	83 after 2000 cycles	10	9(90)	[31]

Table 1. *Cont.*

No.	Material Structure	Electrode Composition (Active:Conductive:Binder) / %	Negative Electrode	Electrolyte	Output Voltage vs. Li$^+$ / V	Capacity Retention / % of Initial Capacity	Current / C	Capacity per Electrode Mass (Polymer mass) / mAh g^{-1}	Ref
40		30:60:10	Li	1 M LiPF$_6$ / EC:DEC	3.6	87 after 170 cycles	0.16	33(110)	[78]
41		100:0:0	Pt	0.1 M TBAClO$_4$ / AN	0.8 vs. Ag/AgCl	99 after 500 cycles	100	70(70)	[45]
42		30:60:10	Li	1 M LiPF$_6$ / EC:DEC	3.6	95 after 50 cycles	0.1	31(104)	[117]
43		10:80:10	Li	0.1 M LiClO$_4$ / EC:DEC	3.67	85 after 100 cycles	5	2(20)	[67]
44		100:0:0	Graphite	0.05 M LiPF$_6$ / DMF:DEC	3.9	n/a	10	39(39)	[79]
45		10:80:10	Li	1 M LiPF$_6$ / EC:DMC:EMC	3.6	90 after 1000 cycles	10	7(65)	[80]
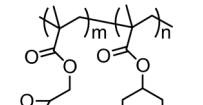
Table 1. *Cont.*

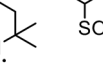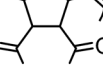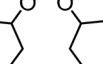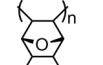| No.	Material Structure	Electrode Composition (Active:Conductive:Binder) / %	Negative Electrode	Electrolyte	Output Voltage vs. Li+ / V	Capacity Retention / % of Initial Capacity	Current / C	Capacity per Electrode Mass (Polymer mass) / mAh g^{-1}	Ref
46		100:0:0	Carbon	0.1 M TBAClO$_4$ / EC:DEC	0.8 vs. Ag/AgCl	90 after 100 cycles	1	103(103)	[28]
47		10:80:10	Li	1 M LiPF$_6$ / EC:DMC	3.62	98 after 50 cycles	1	4 (41)	[81]
48		10:80:10	Pt	0.1 M TBAClO$_4$ / AN	0.7 vs. Ag/AgCl	90 after 1000 cycles	60	7(74)	[118]
49		90:10:0	Pt	0.1 M TBAClO$_4$ / AN	0.7 vs. Ag/AgCl	n/a	10	53(59)	[118]
50		30:60:10	Li	1 M LiPF$_6$ / EC:DEC	3.5	99 after 1000 cycles	10	~23(77)	[24]
51		90:10:0	Li	1 M LiPF$_6$ / EC:DEC	3.5	70 after 200 cycles	1	72(80)	[27]
52		30:60:10	Li	1 M LiPF$_6$ / EC:DEC	3.6	n/a	1	24(80)	[119]
53		95:5:0	Pt	0.5 M (n-C$_4$H$_9$)$_4$NClO$_4$ / AN	0.2 vs. Fc/Fc+	n/a	10	83(87)	[82]

Table 1. *Cont.*

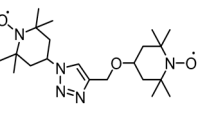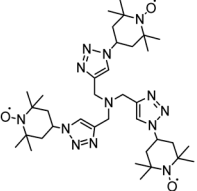| No.	Material Structure	Electrode Composition (Active:Conductive:Binder) / %	Negative Electrode	Electrolyte	Output Voltage vs. Li+ / V	Capacity Retention / % of Initial Capacity	Current / C	Capacity per Electrode Mass (Polymer mass) / mAh g^{-1}	Ref
54		100:0:0	Organic PAQE	3 M NaCl / H_2O	0.7 vs. Ag/AgCl	n/a	18	60(60)	[120]
55		100:0:0	Polyviologen	0.1 M $NaBF_4$ / H_2O	0.7 vs. Ag/AgCl	80 after 2000 cycles	60	110(110)	[19]
56		80:10:10	Li	1 M $LiPF_6$ / EC:DMC	n/a	63 after 100 cycles	1	64(80)	[29]
57		100:0:0	Pt	0.1 M $NaBF_4$ / H2O	0.7 vs. Ag/AgCl	97 after 1000 cycles	60	114(114)	[121]
58		80:10:10	Li	1 M $LiPF_6$ / EC:DMC	n/a	95 after 100 cycles	1	76(96)	[29]
59		100:0:0	Li	1 M $LiPF_6$ / EC:DEC	3.6	99 after 1000 cycles	10	106(106)	[61]
60		10:80:10	Organic	1 M $TBAClO_4$ -TBAOH / AN	0.66	80 after 250 cycles	360	3(32)	[122]
61		10:80:10	Li	1 M $LiPF_6$ / EC:DEC	3.6	90 after 500 cycles	1	11(109)	[123]
62		30:60:10	Li	1 M LiTFSI/EMITFSI	3.5	99 after 100 cycles	1	22(74)	[124]
63		10:80:10	Li	1 M $LiPF_6$ / EC:DEC	3.6	90 after 100 cycles	1	11(107)	[25]
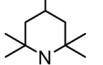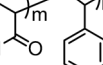
Table 1. *Cont.*

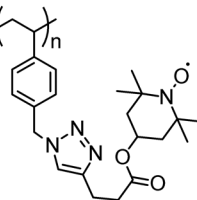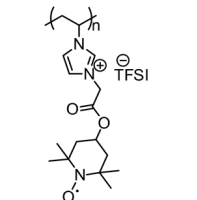| No.	Material Structure	Electrode Composition (Active:Conductive:Binder) / %	Negative Electrode	Electrolyte	Output Voltage vs. Li+ / V	Capacity Retention / % of Initial Capacity	Current / C	Capacity per Electrode Mass (Polymer mass) / mAh g^{-1}	Ref
64		10:80:10	Li	1 M LiPF$_6$ / EC:DEC	3.6	n/a	1	10(93)	[25]
65		40:50:10	Li	1 M LiPF$_6$ / EC:DMC:PC	3.6	80 after 200 cycles	0.5	47(117)	[83]
66		40:50:10	Li	1 M LiPF$_6$ / EC:DMC:PC	3.6	96 after 200 cycles	0.5	35(87)	[83]
67		20:70:10	Li	1 M LiPF$_6$ / EC:DEC	3.6	Stable after 80 cycles	0.25	6.2(31)	[21]
68		100:0:0	Li	1 M LiTFSI / EC:DEC:DMC	3.62	89 after 100 cycles	1	170(170)	[23]

Table 1. *Cont.*

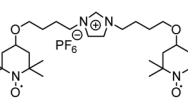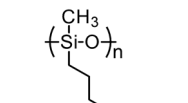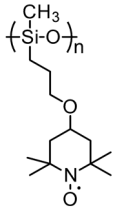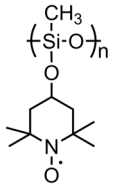| No.	Material Structure	Electrode Composition (Active:Conductive:Binder) / %	Negative Electrode	Electrolyte	Output Voltage vs. Li$^+$ / V	Capacity Retention / % of Initial Capacity	Current / C	Capacity per Electrode Mass (Polymer mass) / mAh g^{-1}	Ref
69		50:50:0	Li	1 M LiTFSI / EC:DEC:DMC	n/a	92 after 3600 cycles	60	35(69)	[84]
70		30:60:10	Li	1 M LiPF$_6$ / EC:DMC	3.5	76 after 300 cycles	1	18(59)	[85]
71		30:60:10	Li	1 M LiPF$_6$ / EC:DMC	3.5	99 after 50 cycles	1	24(80)	[85]
72		40:50:10	Li	0.5 M LiTFSI / EMImTFSI	3.45	98 after 30 cycles	1	32(80)	[86]
73		20:70:10	Li	1 M LiPF$_6$ / EC:DEC	3.6	n/a	0.5	9(46)	[87]
74		20:70:10	Li	1 M LiPF$_6$ / EC:DEC	3.6	99 after 100 cycles	0.5	18(89)	[87]
75	TEMPO-DNA molecule	10:80:10	Li	1 M LiPF$_6$ / EC:DEC	3.6/2.8	90 after 100 cycles	1	6(60)	[125]
76	TEMPO-cellulose	10:80:10	Li	1 M LiPF$_6$ / EC:DEC	3.6/2.8	93 after 110 cycles	1	6(61)	[32]
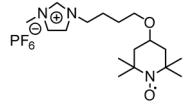
Table 1. *Cont.*

No.	Material Structure	Electrode Composition (Active:Conductive:Binder) / %	Negative Electrode	Electrolyte	Output Voltage vs. Li^+ / V	Capacity Retention / % of Initial Capacity	Current / C	Capacity per Electrode Mass (Polymer mass) / mAh g^{-1}	Ref
77	TEMPO-Carbon	80:15:5	Naphtalimide	1 M TBABF$_4$ / PC	0.9 vs. Ag/Ag^+	70 after 50 cycles	0.1	6(8)	[126]
78	TEMPO-functionalized graphene	80:10:10	Li	1 M LiPF$_6$ / EC:DMC	1.4	n/a	0.6	874(1093)	[127]
79	TEMPO-functionalized graphite nanoplatelet	100:0:0	Li	1 M LiPF$_6$ / EC:DEC:DMC	n/a	n/a	1	450(450)	[128]
80	TEMPO / hollow carbon spheres composite	80:10:10	Li	1 M LiPF$_6$ / EC:DEC:DMC	3.7	82 after 200 cycles	0.5	264(330)	[88]
81	TEMPO-based six-arm star	40:50:10	Li	1 M LiPF$_6$ / EC:DEC	3.6/2.9	n/a	1	13(32)	[89]
82		20:70:10	Li	1 M LiPF$_6$ / EC:DEC	3.6	n/a	1	23(115)	[90]

3.1.2. Redox-Conducting Polymers

As the backbone is usually a non-conjugated polymer, TEMPO-containing non-conductive polymers suffer from low electronic conductivity and require large content of conductive additives, which reduces the practical capacity of the electrode materials. As a result, molecular design of organic electrode materials is aiming at the development of polymers with high specific capacity or better conductivity by varying the nature of the monomeric units and linkers between the polymer framework and active redox groups. An approach based on combining conducting polymers with electroactive groups can increase the conductivity of the materials without their loss of capacity. Intrinsically conducting polymers are defined as macromolecular compounds with a system of conjugated π-bonds in the main chain providing them with electronic conductivity [129,130]. Such a system ensures the conductivity of the material when it is doped with weakly bound ions. The switching of the polymer to its conductive state occurs upon either oxidation (p-doping) or reduction (n-doping), accompanied by doping by an anion or a cation to maintain electroneutrality [131]. For the purpose of discussing TEMPO-based polymers, this review will limit the discussion to p-doped intrinsically conducting polymers. Oxidation potential can be controlled over a wide range by changing the chemical structure of the polymer. Known conjugated polymers may be grouped by structural similarity of the main chain fragments, typically based on polyacetylene, polyphenylene, polyphenylene vinylene, polypyrrole, polythiophene, polyaniline and a few other types of repeat units [129]. The combination of conductive polymers with energy-bearing TEMPO groups in one molecule by grafting approach makes it possible to obtain redox-conductive polymers (RCPs). As will be emphasized below, this strategy yields an intriguingly large variety of structures, which have their pros and cons (Table 2). The optimal performance of RCPs requires perfect matching of the switching potential of the redox-active polymer with redox potential of electroactive groups. This section presents several novel TEMPO-containing RCPs and discusses their electrochemical properties for battery applications.

Polyacetylene is the first discovered conductive polymer with the simplest structure of the conjugated backbone [132]. The short and rigid repeat unit of the polymer limits the possible variations of polyacetylene-based RCPs, which reflects the performance of the obtained materials. A great contribution to the creation of TEMPO- and (2,2,5,5-tetramethylpyrrolidynyl-*N*-oxyl) PROXYL-containing polymers based on acetylene and norbornene was made by Masuda et al. [56]. They compared the properties of four polymers **83–86** with different structures of the TEMPO-bearing linker, discussing structural limitations which hinder utilization of several TEMPO-groups in a single acetylene-based repeat unit. Acetylene-based polymers **83–85** reached 67 mAh g^{-1}, 82 mAh g^{-1}, and 23 mAh g^{-1}, respectively, which indicates poor performance of **85** that contains two neighboring TEMPO groups. To explore the effect of close contact of TEMPO-groups, which emerged in polyacetylene-based polymers, several norbornene-based materials with two TEMPO-groups per monomer unit were synthesized. The norbornene repeat unit allows more structural diversity of the resulting polymers and thus may be used to control the distance between neighboring TEMPO-groups. Polymer **86** was made in two versions: *endo-*, *endo-* and *endo-*, *exo-*orientation of TEMPO groups. Polymer **86** in *endo-*, *exo-*orientation showed five times as high capacity (109 mAh g^{-1}) as polymer **85**. It should be mentioned that the work revealed other similar structures; however, the polymer with a longer linker was too difficult to deposit and it was not possible to examine its charge-storage performance. Conversely, the *endo*, *endo* variant of **86** demonstrated only 54 mAh g^{-1}, which means *endo-*, *exo-*orientation enhanced performance. The authors noted that linker length and distance between TEMPO groups are key variables responsible for material performance. The cationic form of charged TEMPO group can shield neighboring TEMPO group from oxidation and decrease polymer capacity, which is what Masuda observed for polymers **85** and **86** in *endo-*, *endo-*orientation.

Another work [36] indicated a severe influence of helical conformation of polymers on battery performance. The paper compared the properties of five polymers **87–91** with

different structures of the nitroxyl-bearing linker, as well as the properties of TEMPO and PROXYL functional groups. Most of the materials reached their theoretical maximum of the capacity (78.6–112 mAh g^{-1}) except for polymer **87** (43.2 mAh g^{-1}, i.e., only ~33% of theoretical maximum). The authors associated this phenomenon with macroscopic aggregate states, for example, the size and hardness of polymer powders, but not with the spin concentration, since its values for polymers **87** and **88** were comparable. Authors thoroughly studied the one-handed helical structure, which should carry helically arranged TEMPO and PROXYL moieties in the side chain. In this study, only polymers **87**, **88** and **90** had helical structure, and the amide group caused polymer **90** to form a helix. Upon the oxidation of one radical in any of these polymers, a cationic species forms that suppresses further oxidation of the neighboring radicals because of the through-space electrostatic effect. Thus, helical polymers **87**, **88** and **90** exhibited better capacity retention with the increase in current densities than non-helical **89** and **91,** which highlights the importance of the structure of the radical-carrying linker. Although maximum capacity values for polymers were obtained at low current (~1 C), 54% of initial capacity for polymer **6** was shown to be retained at ~70 C, which is excellent performance for electrode materials.

The other eight polymers (**92–99**) with one, two or even four TEMPO groups per monomer unit and a wide variety of linker structure were shown in the paper [133]. The authors discussed the synthesis of TEMPO-containing polyacetylenes by direct polymerization of TEMPO-containing acetylenes with a rhodium-based transition metal catalyst and their electrochemical performance. The capacity of the materials based on polymers **92**, **95** and **96**, containing 80% of carbon fiber, reached 108 mAh g^{-1}, 96.3 mAh g^{-1}, and 89.3 mAh g^{-1}, respectively, corresponding to 100% of their theoretical capacity. It is vital that polymer **94**, which contains four TEMPO groups per unit, had maximum theoretical capacity (106.2 mAh g^{-1}), yet it was not far off for all other polymers. This means that attaching more TEMPO groups per monomer unit is pointless for battery application but can be the key to explaining interactions between adjacent groups. Cyclability was high for all polymers (~85–87% retained after 100 cycles) except **93**. For this polymer, the increase in capacity was observed, which, as authors explained, appears from the increase in the contact surface between the electrode and the electrolyte due to the swelling of the polymer during the charge/discharge process. Polymers **93**, **94**, **97–99** reached 21.3 mAh g^{-1}, 62.3 mAh g^{-1}, 63.0 mAh g^{-1}, 80.5 mAh g^{-1} and 66.0 mAh g^{-1} values, respectively, which are lower than that of the polymer **92**. Considering that the theoretical maximum of capacity for all polymers is ≈110 mAh g^{-1}, the authors attributed the low performance of some polymers to the differences in both molecular structures (e.g., the special arrangement of the TEMPO radicals) and macroscopic aggregation states (e.g., the size and hardness of the polymer powders). Bahceci [134] reported the polyacetylenes (polymers **100**) with TEMPO pendants, with a specific capacity of about 103 mAh g^{-1} at a standard current of ~0.3 C. Upon the current increase to 1.8 C the capacity of the material dropped by ~50% (to 50 mAh g^{-1}) even though the cathode material contained 70% carbon. Battery demonstrated only a fifth of total capacity (~21 mAh g^{-1}) per total cathode mass and showed poor cyclability (62% of initial capacity remained after 40 cycles). The authors emphasized that low performance may be due to inefficient counterion transport and/or electrode material dissolution which can be solved by further polymer modification. Considering these three studies we can conclude that structures **93**, **94** and **97** may suffer from the shielding effect that we described earlier due to high molecule load by neighboring TEMPO groups. Polymers **92** and **93** should have equal electrochemical performance, but an amide group influences TEMPO linkers interaction and keeps suitable distance between them as it was for polymer **90**. Structure **95** seems stiff enough to keep the TEMPO group at a reasonable distance which allows it to gain high material performance. Polymers **98** and **99** are roughly the same as polymer **100** and can suffer from high solubility or instability. At the same time, the incorporation of a bulky group into the linker structure of polymer **96** can stabilize the material, as it does for polymer **88**.

Masuda also conducted another study devoted to the investigation of polyacetylene- and polynorbornene-PROXYL-based materials [135] with similar structures. Another set of six polymers containing one or two PROXYL groups per monomer unit was investigated. The same phenomenon occurred as with TEMPO-containing polymers: the materials reached a high-capacity value of 84.9–117 mAh g^{-1} (78–98% of maximum theoretical capacity), however the stability was about 10% lower than that of TEMPO-containing materials described above, which means no significant gap exists between PROXYL and TEMPO properties. Each nitroxyl radical can be selected for cathodic materials creation depending on required molar mass or volume of pendant groups.

Decent performance of polyacetylene-based polymers promotes application of different conductive backbones to transfer charge to TEMPO groups.

Several polypyrrole-based materials with different TEMPO-bearing linkers were reported by Xu [37]. Polymers **101** and **102** differ only in the length of the linker, which significantly changes the properties of materials. Polymer **102** was able to provide the specific capacity of 115 mAh g^{-1} even with 50% of active material in the composite at low currents (~0.25 C) while **101** reached only 87 mAh g^{-1}. Authors explained that higher capacity of polymer **102** can be attributed to the special arrangement of the TEMPO radicals, which increases the electron migration, and to the fast reaction in the TEMPO-based polymer, leading to the full utilization of the electroactive material. A suitable side-chain length can alleviate torsion between the neighboring pyrrole units in the backbone and enhance the interaction between the pendant radical groups (as proven by UV-vis spectra), resulting in an increased capacity. It was also mentioned that the loose aggregation structure of the polymer **102** particles is in favor of the electrode–electrolyte contact, which can also be attributed to the better utilization of active material and the increase in specific capacity. It is interesting that charge/discharge curves for both polymers contained a second process at 2.7 V, related to the redox transformation from the anionic form of TEMPO into the nitroxyl radical which is evidence of an easier reduction process for TEMPO groups linked with polypyrrole backbone. The same monomer was also subjected to copolymerization with pyrrole at different fed ratios [136]. Using this approach authors obtained copolymers **103** with 4:1 and 8:1 ratios between pyrrole and pyrrole-containing TEMPO group units. These polymers reached 70.9 mAh g^{-1} and 62.6 mAh g^{-1}, respectively. Contrary to previous work, this time cathode materials consisted of 100% polymer. It was hardly possible to reveal a plateau at 3.6 V, commonly observed for TEMPO, which can be due to using carbon substrate characterized by a strong capacitor-like slope of charge/discharge curve. In previous work, authors used a slurry for cathode fabrication which provided negligible substrate signal. Unmodified polypyrrole reached 41 mAh g^{-1} and lost only 2% after 20 discharge cycles. Sample 4:1 lost 24.4% and 8:1 lost 29% of initial capacity value. According to the authors, an open architecture of the modified polymers synthesized with introduction of bulk TEMPO groups results in moderate cycling stability. This leads to the increased instability of the obtained copolymers during the charge/discharge process and hence the decrease in cycling capacity.

The polymer **101** obtained by Xu was also carefully compared with the unmodified polypyrrole [137]. This time the polymer reached the same value of 86.5 mAh g^{-1} (named **104**), which is 4.5 times higher than that of polypyrrole-based cathode (21.7 mAh g^{-1}). The charge/discharge curve of **104** contained the standard plateau at 3.6 V which provided ~50% of the obtained capacity value. This indicates that the part of the polymer backbone participates in the recharging of the hybrid material. This discharge profile is also much more suitable for battery applications than the polypyrrole capacitor-like profile. The polymer **105** was also synthesized by Xu [34] using polyaniline as a conductive skeleton. In this work, copolymers with different ratios of (aniline) and (aniline + TEMPO) fragments (5:1, 3:1 and 1:1) were created. Interestingly, polyaniline itself reached fairly high capacity (94.3 mAh g^{-1}), but had a sloping charge/discharge curve profile, which makes its use in batteries difficult. The addition of TEMPO to the polymer lowered the capacities of the materials to 77.3 mAh g^{-1}, 60.0 mAh g^{-1}, and 44.2 mAh g^{-1} for **105**(5:1), **105**(3:1), and **105**(1:1)

copolymers, respectively. The authors explained that, during the discharge process, the polyaniline backbone is de-doping, entering the de-doped state and becoming an insulator, which severely affects the availability of the active material in the electrode. Considering the absence of a plateau of TEMPO groups on the discharge curves, it can be concluded that, without an active conducting skeleton, TEMPO groups do not participate in charge transfer, which reduces the specific capacity of the composites. TEMPO-containing polyaniline-based polymers were also obtained by Oyaizu (polymer **106**) [138]. Molecules were made by incorporating polyaniline chains into the radical polymer both as the conducting path and the crosslinking moiety, to study the nature of charge transfer and storage processes in the hybrid material. Organic cathodes showed low initial specific capacity (less than 60 mAh g^{-1} compared to PTMA- and PTVE-based cathodes [70,139] with 85–130 mAh g^{-1}) but can work without any carbon additives. Maximum capacity was achieved at high currents of ~10 C, of which up to 50% remained even at 360 C, which testifies to excellent performance of the pure organic cathode. The paper also described several composite materials with various modifications of the main chain, which makes it possible to fine-tune the electrochemical properties of cathode materials. However, the additional load on the monomer unit of the polymer, which significantly reduces the maximum theoretical capacity, should be considered.

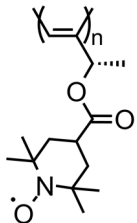**Table 2.** Structures and energy storage performance of the TEMPO-containing polymers with conductive backbones.

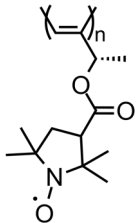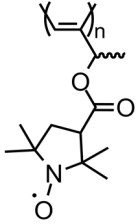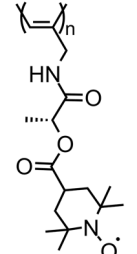| No.	Material Structure	Capacity per Electrode Mass (Polymer Mass) / mAh g^{-1}	E/V	Current / C	Capacity Retention / % of the Initial Value	Electrode Composition / %	Electrolyte	Ref
83		7 (67)	3.58	1	n/a	10 / 80 C / 10 fluorinated polyolefin	1 M LiPF$_6$ EC:DEC (3:7)	[56]
84		8 (82)	3.58	1	n/a	10 / 80 C / 10 fluorinated polyolefin	1 M LiPF$_6$ EC:DEC (3:7)	[56]
85		2 (23)	3.58	1	n/a	10 / 80 C / 10 fluorinated polyolefin	1 M LiPF$_6$ EC:DEC (3:7)	[56]
86		11 (109)	3.58	1	n/a	10 / 80 C / 10 fluorinated polyolefin	1 M LiPF$_6$ EC:DEC (3:7)	[56]

Table 2. *Cont.*

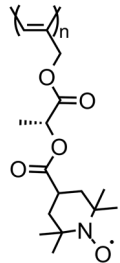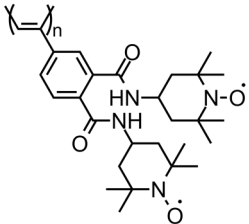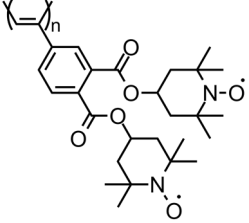| No.	Material Structure	Capacity per Electrode Mass (Polymer Mass) / mAh g^{-1}	E/V	Current / C	Capacity Retention / % of the Initial Value	Electrode Composition / %	Electrolyte	Ref
87		4 (43)	3.6	1	~81 after 100 cycles	10 / 80 C / 10 fluorinated polyolefin	1 M LiPF$_6$ EC:DEC (3:7)	[36]
88		10 (103)	3.6	1	~83 after 100 cycles	10 / 80 C / 10 fluorinated polyolefin	1 M LiPF$_6$ EC:DEC (3:7)	[36]
89		11 (112)	3.6	1	~86 after 100 cycles	10 / 80 C / 10 fluorinated polyolefin	1 M LiPF$_6$ EC:DEC (3:7)	[36]
90		8 (78)	3.6	1	~76 after 100 cycles	10 / 80 C / 10 fluorinated polyolefin	1 M LiPF$_6$ EC:DEC (3:7)	[36]

Table 2. *Cont.*

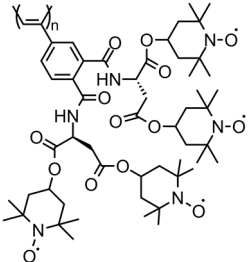| No.	Material Structure	Capacity per Electrode Mass (Polymer Mass) / mAh g^{-1}	E/V	Current / C	Capacity Retention / % of the Initial Value	Electrode Composition / %	Electrolyte	Ref
91		9 (85)	3.6	1	~80 after 100 cycles	10 / 80 C / 10 fluorinated polyolefin	1 M LiPF$_6$ EC:DEC (3:7)	[36]
92		11 (108)	3.6	1	85 after 100 cycles	10 / 80 C / 10 fluorinated polyolefin	1 M LiPF$_6$ EC:DEC (3:7)	[133]
93		2 (21)	3.6	1	n/a	10 / 80 C / 10 fluorinated polyolefin	1 M LiPF$_6$ EC:DEC (3:7)	[133]

Table 2. *Cont.*

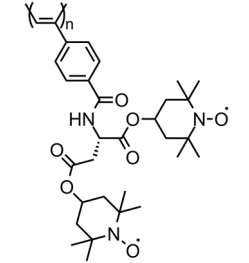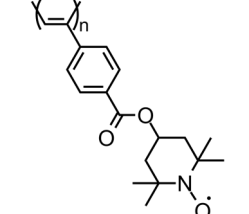| No.	Material Structure	Capacity per Electrode Mass (Polymer Mass) / mAh g^{-1}	E/V	Current / C	Capacity Retention / % of the Initial Value	Electrode Composition / %	Electrolyte	Ref
94		6 (62)	3.6	1	n/a	10 / 80 C / 10 fluorinated polyolefin	1 M LiPF$_6$ EC:DEC (3:7)	[133]
95		10 (96)	3.6	1	~88 after 100 cycles	10 / 80 C / 10 fluorinated polyolefin	1 M LiPF$_6$ EC:DEC (3:7)	[133]
96		9 (89)	3.6	1	~86 after 100 cycles	10 / 80 C / 10 fluorinated polyolefin	1 M LiPF$_6$ EC:DEC (3:7)	[133]

Table 2. *Cont.*

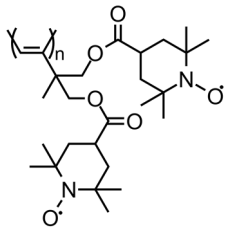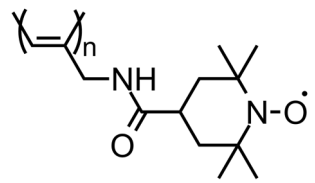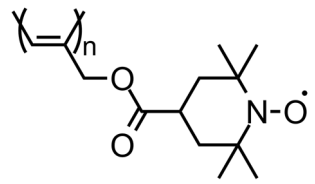| No.	Material Structure	Capacity per Electrode Mass (Polymer Mass) / mAh g^{-1}	E/V	Current / C	Capacity Retention / % of the Initial Value	Electrode Composition / %	Electrolyte	Ref
97		6 (63)	3.6	1	~87 after 100 cycles	10 / 80 C / 10 fluorinated polyolefin	1 M LiPF$_6$ EC:DEC (3:7)	[133]
98		8 (81)	3.6	1	n/a	10 / 80 C / 10 fluorinated polyolefin	1 M LiPF$_6$ EC:DEC (3:7)	[133]
99		7 (66)	3.6	1	n/a	10 / 80 C / 10 fluorinated polyolefin	1 M LiPF$_6$ EC:DEC (3:7)	[133]
100		21 (103)	3.61	0.3	62 after 40 cycles	20 / 70 C / 10 PVDF	1 M LiPF$_6$ EC:DEC (1:1)	[134]

Table 2. *Cont.*

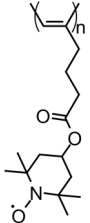| No.	Material Structure	Capacity per Electrode Mass (Polymer Mass) / mAh g^{-1}	E/V	Current / C	Capacity Retention / % of the Initial Value	Electrode Composition / %	Electrolyte	Ref
101		44 (87)	3.6	0.25	55 after 50 cycles	50 / 40 C / 10 PVDF	1 M LiPF$_6$ EC:DMC (1:1)	[37]
102		58 (115)	3.6 / 2.7	0.25	75 after 50 cycles	50 / 40 C / 10 PVDF	1 M LiPF$_6$ EC:DMC (1:1)	[37]
103		n. a. (71)	3.6	0.25	76 after 20 cycles	100	1 M LiPF$_6$ EC:DMC (1:1)	[136]
104		44 (87)	3.5	0.25	~56 after 50 cycles	50 / 40 C / 10 PVDF	1 M LiPF$_6$ EC:DMC (1:1)	[137]

Table 2. *Cont.*

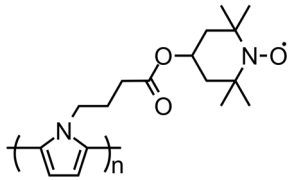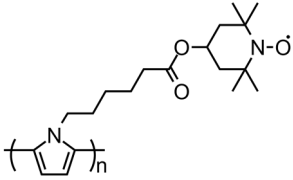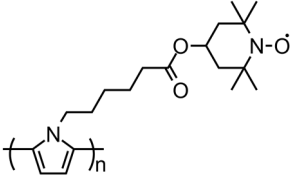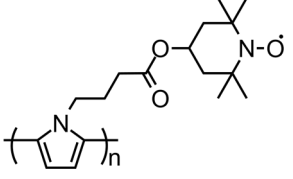| No.	Material Structure	Capacity per Electrode Mass (Polymer Mass) / mAh g^{-1}	E/V	Current / C	Capacity Retention / % of the Initial Value	Electrode Composition / %	Electrolyte	Ref
105		39(77)	3.6	0.2	19 after 20 cycles	50 / 40 C / 10 PVDF	1 M LiPF$_6$ EC:DMC (1:1)	[34]
106		~60 (60)	0.8 (vs. SCE)	10	n/a	100	0.1 M TBAClO$_4$ CH$_3$CN	[138]
107		68 (135)	3.82	0.15	90 after 100 cycles	50 / 40 C / 10 PVDF	1 M LiPF$_6$ EC:DEC	[140]
108		70(140)	3.6	1	89 after 50 cycles	50 / 40 C/ 10 PVDF	1 M LiPF$_6$ / EC:DEC	[41]

Table 2. *Cont.*

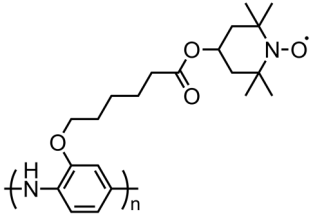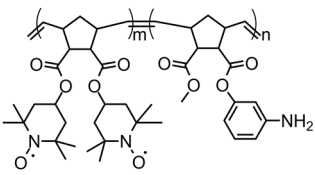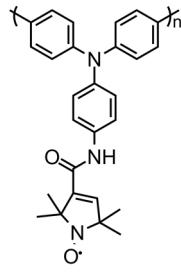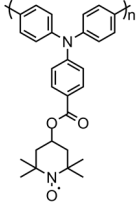| No.	Material Structure	Capacity per Electrode Mass (Polymer Mass) / mAh g^{-1}	E/V	Current / C	Capacity Retention / % of the Initial Value	Electrode Composition / %	Electrolyte	Ref
109		24 (79)	3.6	0.1	77 after 50 cycles	30 / 60 C / 10 PVDF	1 M LiPF$_6$ EC:DEC	[33]
110		22 (89)	3.65	1	87 after 9 cycles	25 / 65 C / 10 PVDF	1 M LiPF$_6$ EC:DEC	[141]
111		68 (68)	3.6	~0.5	n/a	100	0.5 M LiClO$_4$ PC	[39]
112		44 (44)	3.6	~0.5	n/a	100	0.5 M LiClO$_4$ PC	[39]
113		22 (22)	3.6	~0.5	n/a	100	0.5 M LiClO$_4$ PC	[39]
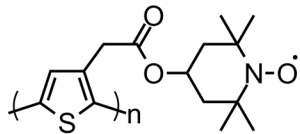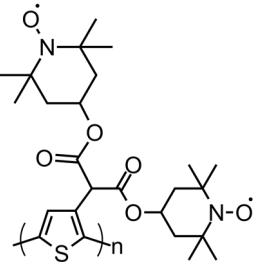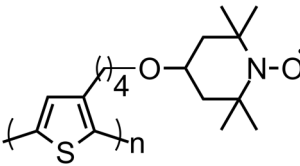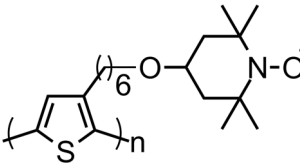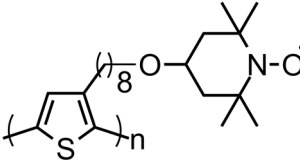
Table 2. *Cont.*

No.	Material Structure	Capacity per Electrode Mass (Polymer Mass) / mAh g^{-1}	E/V	Current / C	Capacity Retention / % of the Initial Value	Electrode Composition / %	Electrolyte	Ref
114		~65 (65)	3.61	3	70 after 200 cycles	100	0.5 M LiClO$_4$ PC	[75]
115		36 (47)	3.62	0.1	81 after 50 cycles	77 / 33 C	1 M LiPF$_6$ EC:DMC	[40]
116		n. a.	3.6	0.1–5	n/a	70 / 30 C	1 M LiPF$_6$ EC:DMC	[142]
117		20 (50)	0.36 (vs. Fc+/Fc)	1	93 after 6 cycles	40 / 40 C / 20 PVDF	1 M LiPF$_6$ EC:DMC (1:1)	[143]
118		82 (82)	0.53 (vs. Ag | AgNO$_3$)	60	90 after 100 cycles, 66 after 2000 cycles	100	0.1 M Et$_4$NBF$_4$ / CH$_3$CN	[42]
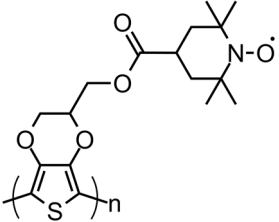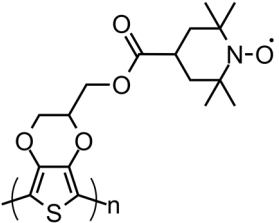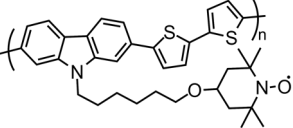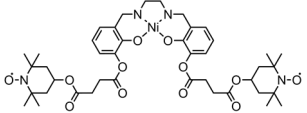
Polymer **107** derived from nitroxyl-modified triphenylamine by Xiong [140] reached a specific capacity of 135 mAh g^{-1} with high cycling stability and retained ~67% of the initial value at higher currents (~4 C). This result is, however, determined mostly by the high capacity of poly(triphenylamine) itself (101 mAh g^{-1}), while the nitroxyl pendants increased the capacity by 25% and stability by 5%. The authors attributed the improved rate capability and cycle stability to the novel chemical structure that combines the conducting polymer backbone and the nitroxide radical pendant. This improves electron transport properties. A similar structure **108** [41] achieved the same values of capacity and stability, which confirms the equivalence of the properties of TEMPO and PROXYL groups.

Like pyrrole, thiophene-based polymers are widely used for synthesis of nitroxyl-containing RCPs. TEMPO-thiophene polymer **109** with an ester linker between conjugated backbone and nitroxyl pendants reported by Aydin [33] delivered a specific capacity value of 79 mAh g^{-1} (~87% of maximum theoretical capacity) which dropped to 38.1 mAh g^{-1} upon current raise to ~20 C. Like in the cases of polymers **101** and **102**, discharge curves for **109** also contained a small slope related to anion-nitroxyl radical reaction at 2.7 V, which indicated the catalytic effect of the conductive backbone. The stability of the material was relatively high (77% remains after 50 cycles at 0.1 C) at low discharge rates and rose at high current (92% remains after 55 cycles at 10 C). Authors explained that the drop in the specific capacity may be attributed to the structural changes occurring in the cathode material, the partial dissolution of the polymer or linkers detaching after extensive cycling. This is also supported by strong distortion of cyclic voltammograms and the appearance of the irreversible oxidation/reduction processes at the edges of the potential window at low scan rate. An introduction of the second TEMPO fragment into a single thiophene unit increased the capacity by 20% [141]. Polymer **110** reached 88.8 mAh g^{-1} (~82% of theoretical maximum) capacity at 1 C, 47% of which remained at 4 C. The authors also associated lower discharge capacity utilization, compared to the full theoretical capacity, with the inability for simultaneous electrochemical oxidation of both the neighboring TEMPO groups and slow counterion diffusion into the composite.

An unusual internal electron transfer in the TEMPO-polythiophenes with different linkers was examined by Li, indicating the key role of the linker in its energy storage performance [39]. In this work authors obtained a family of polythiophenes bearing nitroxide radical groups that differ by linker's length (polymers **111–113**). It was shown that, while both backbone and TEMPO species are electrochemically active, there exists an internal electron transfer mechanism that destabilizes the polymer's fully oxidized form. At low current of ~0.5 C polymers **111**, **112** and **113** reached capacities of 68.0 mAh g^{-1}, 44.0 mAh g^{-1} and 21.5 mAh g^{-1}, respectively, which is only ~15–38% of their theoretical maximum. The same observations were made for polythiophene modified by n-butyl linker with no TEMPO (P3HT, 40.5 mAh g^{-1}, ~21.1% of theoretical value). This indicates that the polythiophene backbone either suppresses or does not enhance redox activity of TEMPO. Estimation of the conductivity of modified polymers revealed a decrease in conductivity by 2–3 orders of magnitude for **111**, **112** (8.1×10^{-7} and 3.6×10^{-7} S cm^{-1}) and by 5 orders for **113** (6.2×10^{-9} S cm^{-1}) compared to a polymer P3HT (1.6×10^{-4} S cm^{-1}). Authors mentioned that higher oxidation potential is required for polythiophenes to switch from the insulating to the conductive form, but the reverse is not required for the reduction process. Thus, the conductivity differences between materials **111** and **113** and their precursor may be a consequence of the internal electron transfer process. The lower conductivity in **113** is due to the longer alkyl spacer that affected the packing of the polymer chains. VIS-spectroelectrochemical methods revealed the decay at open circuit potential via rapid de-doping of the polythiophene backbone caused by internal transfer of an electron from the nitroxide group to the polythiophene backbone. At 4.2 V, the majority of nitroxide radicals and polythiophene backbone are oxidized and doped. A small amount of unoxidized TEMPO remains, because the oxidation reaction does not proceed to full completion. This remainder is capable of transferring one electron to reduce the doped polythiophene

backbone (Figure 8A). Thus, after charging the electrode the polymer potential decays as the polythiophene backbone is reduced by some non-oxidized nitroxides, leading to the de-doping of the backbone and a reduction in conductivity. Open circuit potential relaxation of **111–113** showed one-step voltage decay from the charged state at 4.2 V to 3.6 V, and for precursor polythiophene from 4.2 V to 3.8 V. Since the redox potential (3.60 V) of the radical unit was below that of the conjugated backbone (3.88 V), spontaneous reduction of polythiophene cations by nitroxide radicals is thermodynamically favored. These results explain why conjugated radical polymers **111–113** have exhibited such poor capacity. Authors concluded that reversing or equalizing potentials of two active moieties might provide alternative handles to adjust the stability and capacity of materials.
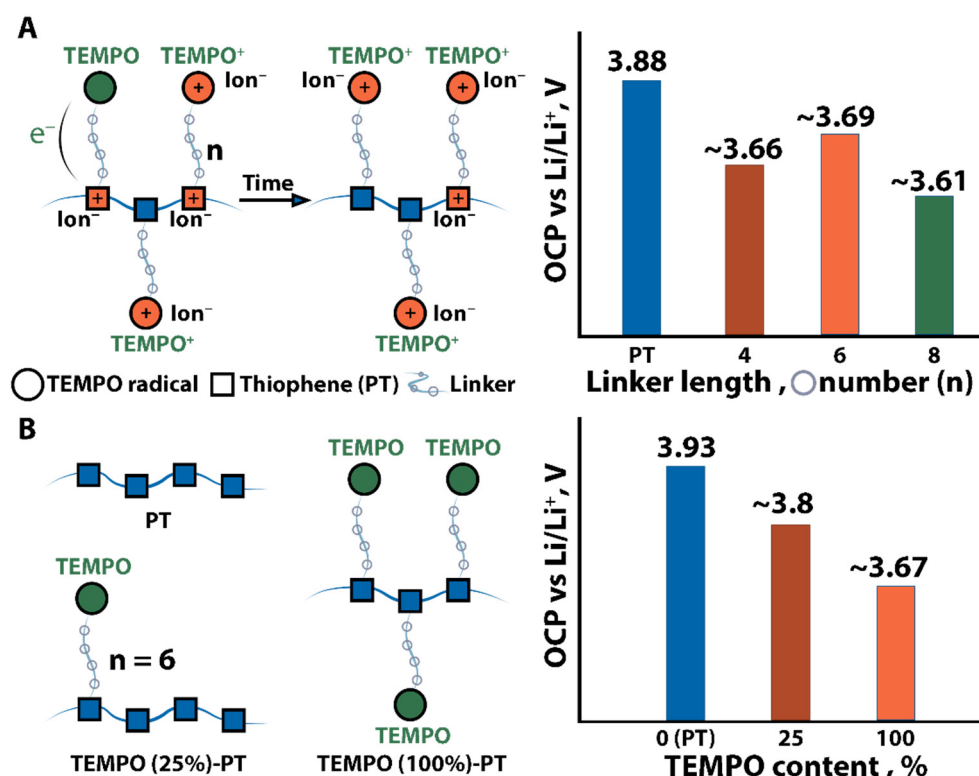
Figure 8. Schematic illustration of the internal charge transfer mechanism for TEMPO-containing polythiophenes depending on linker length (**A**) and TEMPO content (**B**).

Another paper related to these samples [72] also demonstrated the dependence of electrochemical performance on the monomer structure. Polymer **112** exhibited the highest electrochemical activity, whereas **111** showed the highest electron conductivity. It was also noticed that longer octyl chain spacers in **113** suppressed aggregations during electropolymerization and changed surface morphology of **111** from a spherical one to the smoothest film surface. The work [48] describes the internal electron transfer behavior for copolymers of different compositions **111** (25%) (with one TEMPO per four monomer units) and **111** (with one TEMPO per monomer unit). A cyclic voltammogram for polymer with no TEMPO (pP3HT) exhibited one oxidation peak at 3.84 V and two reduction peaks at 3.80 V and 3.36 V; **111** showed a reversible redox couple at 3.68 V (or plateau from 3.6 to 3.7 V in charge/discharge curves). It is crucial that **111** (25%) displayed mixed behavior, in which a rectangular capacitive response was superimposed on a redox peak (3.69 V). As the TEMPO loading increased from **111**(25%) to **111**, the CV peaks became sharper, reflecting that the charge transfer mechanism switched from delocalized polaronic mode to localized electron hopping between the discrete redox centers. In **111**, electron transfer occurs via hopping between adjacent TEMPO sites, because the bulky TEMPO radicals obstruct polymer packing, which prevents charge transfer along the conjugated polythio-

phene backbone. When the radical loading is low, the bulky TEMPO groups are spatially distant, which permits partial charge transfer through the conjugated backbone.

To confirm the difference in TEMPO loading, Zhang [35] measured the radical concentration in the **111** (25%) and **111** using electron paramagnetic resonance (EPR). Material **111** (25%) showed a hyperfine-induced triplet, indicating that the TEMPO radicals are distributed through the polymer chain and local radical concentration is low. On the contrary, **111** showed a broad EPR peak resulting from spin–spin interactions between neighboring TEMPO radicals. Li et al. noted that in the series pP3HT—**111** (25%)—**111**, the maximum theoretical capacity is ≈160 mAh g^{-1}, but the actual capacity, as well as conductivity, decreased. The charge/discharge behavior of materials with gradually increasing oxidation potential revealed that **111** reached more capacity when charged up to 3.8 V than up to 4.2 V, which is evidence of internal charge transfer. Again, open circuit potential relaxation shows a rapid drop in potential for **111** that reflects internal charge transfer from the nitroxide radical to the conjugated polythiophene backbone (Figure 8B). There is no sharp potential decay in the case of **111** (25%), because unoxidized TEMPO radicals reduce only a small amount of the polythiophene, and the polythiophene backbone remains in the doped state for the most part. As a result, the open circuit potential decayed faster than that for pP3HT, but the potential still stabilized near the redox potential of polythiophene (3.8 V), indicating that internal charge transfer is limited by the concentration of un-oxidized TEMPO units.

To further develop this theory and solve the problem of the internal charge transfer Li created a polymer **114** using dithieno[3,2-b:2′,3′-d]pyrrole (DTP) monomers [75], which has lower redox potential (3.15 V) than both thiophene (3.88 V) and the nitroxyl radical (3.61 V). Polymer **114** reached a specific capacity as high as 65 mAh g^{-1} (~47% of theoretical capacity) in 100% polymer cathode. Polymer also had remarkable stability in thin film (~70% remains after 200 cycles), but addition of TEMPO groups in monomer units decreased the Coulombic efficiency by 8% due to the internal charge transfer mechanism mentioned above. Non-modified pDTP exhibited only a sloping discharge profile due to the pseudocapacitive nature. However, pDTP reached 85.1 mAh g^{-1} (~70% of theoretical capacity) and only 50% remained after 200 recharge cycles. This time, as the DTP moiety has a lower oxidation potential (3.15 V) than the TEMPO radical (3.61 V), it was expected of DTP to be electronically conductive during the TEMPO radical oxidation step which was proved by impedance spectroscopy. It was shown that open circuit potential relaxation of **114** indicated two-step voltage decay from the charged state at 4.1 V to 3.6 V and to 3.0 V. For pDTP, only one voltage drop was observed from 4.1 V to 3.0 V (Figure 9). Thus, this situation is the reverse case of **111**–**113**. Authors concluded that upon charging, the DTP unit transfers an electron to the radical, essentially "quenching" the activity of the polymer **114**. This is further manifested by its lower Coulombic efficiency. Li mentioned that this problem might be overcome by matching the redox potentials of the conjugated backbone and the radical groups, thus removing the propensity for internal electron transfer.
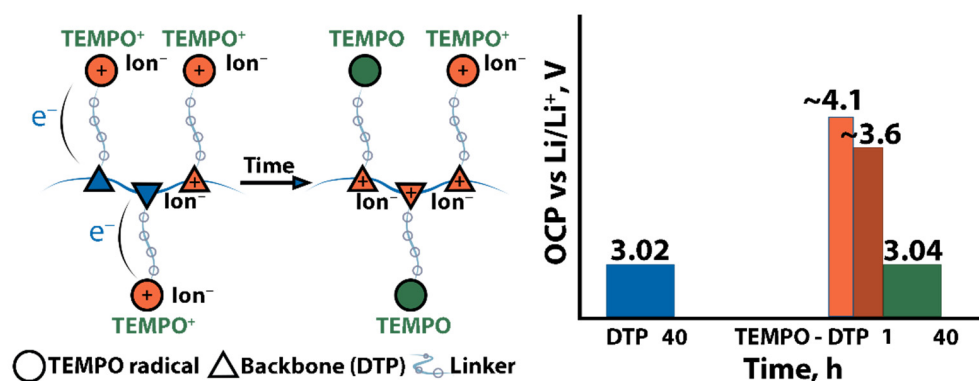

Figure 9. Schematic illustration of internal charge transfer mechanism for TEMPO-containing DTP.

The utilization of 3,4-ethylenedioxythiophene (EDOT)-based monomers, known to form more stable polymers, reduced the specific capacity of the corresponding RCPs with minor increase in stability and discharge rates [40]. Schwartz presented polymers obtained using various oxidizing agents. The polymer **115** obtained using $FeCl_3$ showed poor electrochemical performance, and even after prolonged charging (380 mAh g^{-1}), the polymer did not exhibit any discharge capacity which was associated with the corrosion process with the remaining $FeCl_4^-$ complexes. The use of $Cu(BF_4)_2$ allowed attainment of polymers with 47 mAh g^{-1} (62% of the theoretical capacity) capacity which slightly dropped to 38 mAh g^{-1} after 50 discharge cycles. All cathodes contained 33.0 wt% of carbon black. Since the poly(3,4-ethylenedioxythiophene) (PEDOT) polymer backbone by itself has high electronic conductivity, the electrodes without additional conductive additives were also prepared. The capacity decreased to 20 mAh g^{-1} which indicated that not every TEMPO unit takes part in the cycling process. Electronic connection of the TEMPO groups was not sufficient to exploit the full capacity of RCP. Authors also tried to obtain monomers with two neighboring TEMPO groups. Unfortunately, during the polymerization process, it was not possible to obtain any solid products. As it was explained, the two sterically demanding TEMPO substituents cause a notable steric hindrance at the polymerizable EDOT unit which leads to soluble oligomeric formation. The performance of the same PEDOT-TEMPO material as a conductive binder in $LiFePO_4$ cathodes was tested by Casado [142] and compared to its counterpart cathode containing a conventional binder. Good cycling stability with high Coulombic efficiency and increased cyclability at different rates were obtained using **116** as a replacement of two ingredients: conductive carbon additive and polymeric binders. Best performance was obtained for cathode configuration with 85% LFP / 5% C / 10% polymer **116**. Thus, **116** can replace the conventional binder and reduce the amount of carbon additives that commonly improve electrical conductivity in insulating cathode materials.

Assumma [143] reported a new RCP **117** based on a polymer of 2,7-bisthiophene carbazole (2,7-BTC). This backbone was chosen due to its oxidation potential at 3.7 V, which is close to the redox potential of the TEMPO moiety and has good conductivity. Material reached capacity ~50 mAh g^{-1} which is close to the theoretical maximum (~53 mAh g^{-1}) with a perfect coulombic efficiency of 97%. This copolymer also loses only 20% of capacity at 10 C, and 40% at 20 C. Another example of good redox matching between two moieties is Salen-based TEMPO-containing polymer **118** [42]. The polymer also reached 99% of theoretical capacity (91.5 mAh g^{-1}) 86% of which remained even at 800 C. High performance also indicates that adjacent TEMPO groups are sufficiently spaced from each other to not interfere with mutual oxidation. Conductivity measurements showed perfect matching of Salen-type backbone electroactivity window (3.4–3.8 V) with activity of TEMPO groups (3.6 V) which confirms the Li hypothesis. Despite high cyclability (66% capacity remains after 2000 cycles) authors mentioned the low ability of **118** to form thick layers, which complicates the commercialization of such polymers. This may be due to the use of succinyl linkers containing four oxygen atoms, which prevents polymer packing. The replacement of the linker is a viable path to improve this RCP.

Summing up, redox-conducting polymers have an immense potential for their use as electrode materials. A variety of conductive polymers and TEMPO-supporting linkers allows for fine-tuning of the electrochemical properties of material. However, such a variety of structures impedes the understanding of the functioning of hybrid materials. It was shown that the properties of the material are affected both by the structure of the linker, its rigidity, composition, its length, and the nature of the conductive polymer, the potential of its electrical activity window, rigidity, and its solubility. The difficulty is that the linker composition selected for one system may not be suitable for another at all. Moreover, the same system can yield different results from case to case, which hinders the development of theoretical models of the functioning of hybrid systems. Despite this, there is a possibility of finding an ideal system that will allow the creation of environmentally friendly, fast-charging organic batteries.

3.2. Redox Flow Batteries

Redox polymers are considered as promising electrolyte materials for flow batteries (Figure 10). The main advantage of the polymeric materials is high molecular weight ensuring high enough geometrical dimensions to allow the use of microporous membranes instead of ion-conductive ones to prevent the crossover of electrolyte material and thus increase the ionic conductance between the cell compartments and decrease the price of the target device. TEMPO-containing polymers (Table 3) meet the requirements as catholytes materials due to high potential and fast redox kinetics.
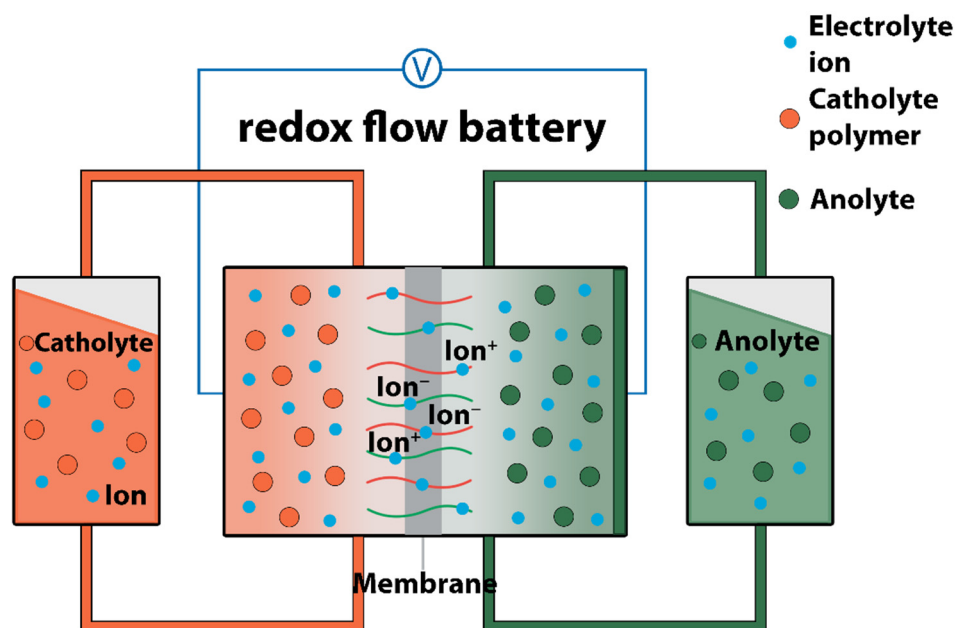
Figure 10. Schematic illustration of a polymer-based redox flow battery.

The water-soluble copolymer of TEMPO methacrylate and choline methacrylate **119** as a catholyte was used with the methyl viologen anolyte and chloride-exchange membrane in all-organic aqueous redox flow cell [144]. The capacity of the catholyte comprises 8.3 Ah L^{-1}. Introduction of the zwitterionic functionality instead of the cationic one significantly increases the solubility of the polymer and decreases the viscosity of the catholyte, affording catholyte **121** with volumetric capacity as high as 20 Ah L^{-1} [145].

In 2015, Janoschka et al. reported an aqueous all-polymer redox flow battery with a water-soluble copolymer of TEMPO methacrylate and choline methacrylate **120** as a catholyte material, a viologen-containing cationic polymer as an anolyte material and cellulose membrane [146]. The capacity of the TEMPO-polymeric catholyte reached the value of 10 Ah L^{-1} and the devices were functional at current densities of up to 40 mA cm^{-2}. The authors also demonstrated that the nature and fraction of the solubilizing comonomer in the polymer has a dramatic influence on its solubility in water and rheological characteristics, which directly determine the energy and power density of the cell [147].

Table 3. Structures and energy storage performance of the TEMPO-polymeric catholytes for redox flow batteries.

No.	Catholyte Polymer Structure	Anolyte	Volumetric Capacity of Catholyte / Ah L^{-1}	E/V (Ag / AgCl)	Current / mA cm^{-2}	Ref
119		Methyl viologen	8.3	0.7	5	[144]
120	Same	Viologen-containing polymer	10	0.7 (Ag/AgCl)	40	[146]
121		Methyl viologen	20	0.7	8	[145]
122		Zn^{2+}/Zn	-	-	-	[148]
123	TEMPO-containing acrylate microgel	-	0.1	-	-	[149]
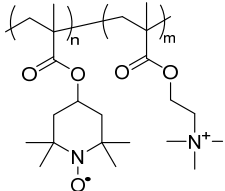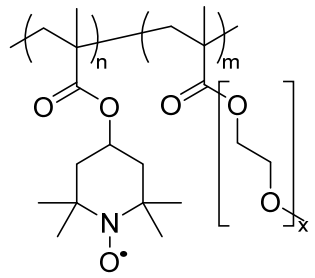
Table 3. *Cont.*

No.	Catholyte Polymer Structure	Anolyte	Volumetric Capacity of Catholyte / Ah L^{-1}	E/V (Ag / AgCl)	Current / mA cm^{-2}	Ref
124	nanoparticles	Viologen polymer or diazaanthraquinone polymer	7.2	-	-	[150]
125		Zn^{2+}/Zn	1.2	0.4 (Ag/AgNO$_3$)	3	[151]
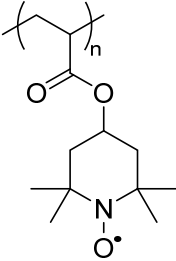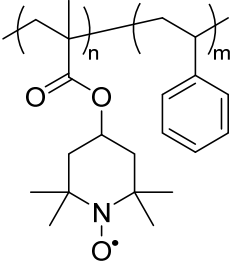
A series of cationic and PEGylated TEMPO-methacrylate copolymers **122** were tested as a catholyte materials in hybrid flow batteries in combination with the Zn^{2+}/Zn anode [148]. In the carbonate-based electrolytes, the cell with the PEGylated polymer attained an impressive overall energy up to 8.1 Wh L^{-1} with 1.7 V cell voltage at a 50% state of charge. In aqueous electrolytes, however, only 4.1 Wh L^{-1} was obtained.

Colloidal anolytes based on TEMPO-containing polymers were also employed in the redox flow batteries. Compared to the solutions of linear polymers, compact micellar and microgel particles provide the solutions with much lower viscosity and lower crossover through microporous membranes. Low-viscosity electrolytes based on hydrophilic TEMPO-acrylate microgels **123** were reported with the capacity of 0.1 Ah L^{-1} [149]. Using the hydrophobic nanoparticles of TEMPO-polyacrylate **124**, the reasonable capacity of 7.2 Ah L^{-1} and cell voltage of 1.1 V were achieved in a full cell with the viologen polymer anolyte [150]. The diazaanthraquinone polymer as anolyte affords an increased voltage of 1.3 V but a lower capacity of 6 Ah L^{-1}.

Core-corona micellar carbonate-based catholyte with copolymer of TEMPO-methacrylate with styrene as active material **125** was also studied in a full cell with the Zn^{2+}/Zn anode [151]. The capacity of the catholyte, limited by a solubility of the copolymer, was estimated as 1.2 Ah L^{-1} at a current of 2 mA cm^{-2}, and the maximum current for the cell was 5 mA cm^{-2}.
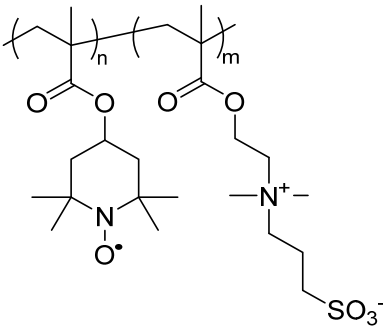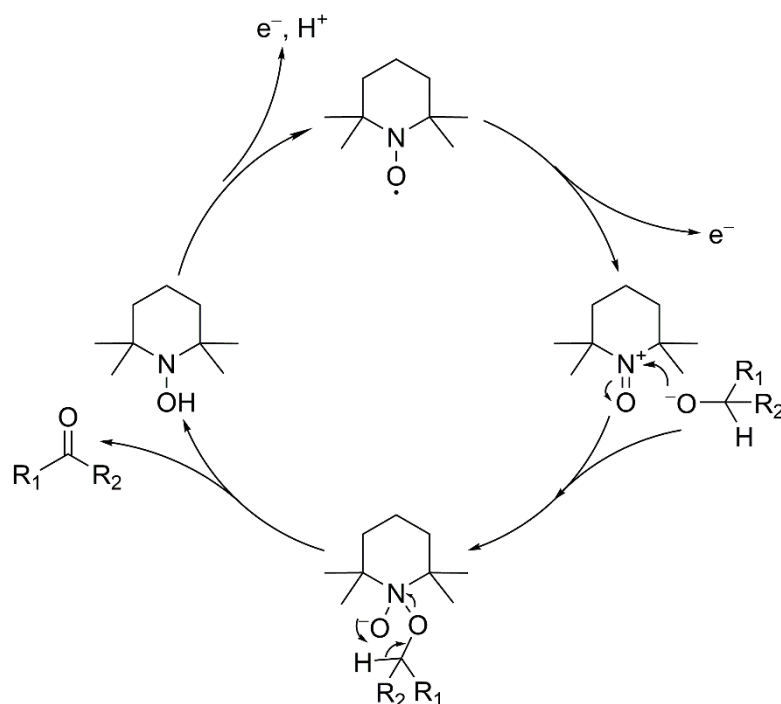
3.3. Catalytic Mediators

Nitroxyl compounds, and primarily TEMPO derivatives, are widely used as two-electron redox mediators for selective oxidation of various organic substrates for analytic or preparative applications. The oxoammonium form of TEMPO contains an electrophilic nitrogen atom, to which different nucleophiles such as alcohols or amines can attach (Figure 11). While the substrate contains an alpha-hydrogen atom, the subsequent proton shift and oxidative elimination of the TEMPO in hydroxylamine form may occur, which results in a formal 1,2-dehydrogenation of the substrate (Figure 11). The catalytic cycle can then be closed by two-electron oxidation of the hydroxylamine form to oxoammonium form using chemical oxidants. As an alternative, the mediator may be regained by electrochemical oxidation by using dissolved or on-electrode TEMPO-containing polymers. This approach secures sufficient electron transfer from an electrode to the TEMPO fragments and excludes the possibility of adverse chemical reactions with chemical oxidants. However, among the works devoted to the homogeneous and solid phase-supported TEMPO-derived redox mediators for electrochemical oxidation of organic substrates [152], the use of TEMPO-modified polymers is much less studied.

3.3.1. Oxidation of Alcohols

Primary and secondary alcohols are the most popular substrates for TEMPO-mediated oxidation, affording aldehydes and ketones, respectively. Catalytic amounts of Brønsted base are commonly added to deprotonate the alcohol, which facilitates its nucleophilic addition to the oxoammonium cation. The oligomeric (M_w ~ 2700 Da) PTMA was used as a homogeneous redox mediator for the oxidation of various primary and secondary alcohols in aqueous acetonitrile solutions [153] in the presence of quaternary ammonium polyelectrolyte. The comparison of electrocatalytic activity in benzyl alcohol oxidation has shown that PTMA surpasses monomeric TEMPO. Polymeric mediator has an additional advantage against TEMPO since it can be easily removed from the reaction mixture and recycled via the membrane filtration. In subsequent work [14], the same authors compared the electrochemical activity of TEMPO, PTMA and 4-acetoxy-TEMPO (ACT) in oxidation of 4-methoxybenzyl alcohol. Although PTMA and ACT have similar redox potential and the redox potential of TEMPO is lower, it was found that ACT has the highest activity among these nitroxyl mediators.

Figure 11. Catalytic cycle of the TEMPO-mediated oxidation of alcohol.

A bifunctional TEMPO-modified poly(ethyleneimine) (TEMPO-LPEI), which serves both as a redox mediator and a basic catalyst, was studied for the electrochemical oxidation of different alcohols and carbohydrates, including methanol, ethanol, isopropanol, glycerol, fructose, and sucrose [30]. Compared to the 4-methoxyTEMPO, in aqueous phosphate buffer electrolyte with pH = 7, oxidation current densities tended to be dramatically higher in the case of TEMPO-LPEI. The same polymer combined with oxalate decarboxylase were immobilized on multi-walled carbon nanotubes (MWCNTs) to construct the system capable of the enhanced oxidation of glycerol [154]. Introduction of enzyme to the system increases the oxidation current at 0.7 V (vs. Ag/AgCl) several times. In combination with alcohol dehydrogenase and aldehyde dehydrogenase enzymes, TEMPO–LPEI provides complete oxidation of ethanol to CO_2 at constant potential electrolysis [155].

To achieve sufficient stability and charge transport during the on-electrode oxidation of alcohols, TEMPO-modified polymers with conductive backbones are used. Several electrochemically deposited TEMPO-modified polypyrrole polymers were reported for an oxidation of the benzyl alcohol to benzaldehyde, catalyzed by 2,6-lutidine [38,156]. TEMPO-modified polythiophene [157], poly(terthiophene) [158] and poly(carbazole) [159] derivatives also demonstrate an electrocatalytic activity towards an oxidation of benzylic alcohol in CH_3CN in a presence of 2,6-lutidine. Interesting example of the enantiospecific oxidation of the 1-phenylethanol on the electrodes coated with polypyrrole, modified with chiral nitroxyl radical SPIROXYL [160]. The ratio of oxidation currents for enantiomeric 1-phenylethanols differs by than 2.5 times. Using this discrimination, an amperometric method for determination of the enantiomeric composition of 1-phenylethanol was proposed.

TEMPO-modified conductive polymers are also suitable for on-electrode oxidation of biorelevant alcohols. In 2010, Ono et al. [161] reported an electrochemically deposited TEMPO-modified polypyrrole, which serves for the oxidation of geraniol to geranial. To facilitate oxidation via the deprotonation of the -OH group, 2,6-lutidine was added as a Brønsted base. A film deposited by a cooperative electrochemical polymerization of 2,2′-dithiophene and TEMPO-modified pyrrole, containing pendant TEMPO group, with 2,2′-bitiophene, exhibited higher oxidation currents in the same system [162]. Oxidation currents of the geraniol with both polymers were found to be linear in relation to the substrate concentration in a wide range, which provides the possibility for the amperometric

sensing of geraniol. Oxidation of carbohydrates on the electrode coated with TEMPO-modified polypyrrole showed the same behavior, which provides the possibility for their amperometric determination [163].

3.3.2. Oxidation of Amines

TEMPO-modified polymers can also catalyze oxidation of amines. Polyamine-immobilized piperidinyl oxyl electrode coating mediates an electrocatalytic oxidation of benzylamine [164]. The same activity was shown for the TEMPO-modified poly acrylic acid and methacrylate, which was found to oxidize the primary amines with alpha-hydrogen atoms to nitriles [165,166]. The abovementioned conductive copolymer of TEMPO-pyrrole and 2,2′-ditiophene can also catalyze the oxidation of primary and secondary amines, as was shown in [167].

4. Conclusions and Prospects

Research focused on design of polymers, containing free nitroxyl radicals, to be used as active materials of batteries and hybrid supercapacitors provided various unique materials based on conjugated and non-conjugated backbones. The specific capacities of most of the materials are close to 100 mAh g^{-1}, which can hardly be improved by molecular design due to high molecular mass of nitroxyl-containing fragments. Therefore, most researchers are focused on improvement of the rate capability and conductivity of the materials. It can be tuned not only by the backbone nature, but also by linker length and configuration, which strongly influences charge transfer between TEMPO fragments. Proper choice of linker length and mobility allows high charge transfer rates even for polymers with aliphatic backbones. Surprisingly, using a conductive backbone does not necessarily lead to better performance of TEMPO-containing materials, because in this case a key role of the redox-matching between the backbone and pendant groups emerges. The redox potentials of the radical and the conjugated backbone should be close enough; otherwise the spontaneous oxidation/reduction between molecule parts is thermodynamically favored, resulting in poor capacity and conductivity of materials.

In contrast to charge storage materials, catalytic activity of TEMPO-based polymers is much less studied. However, existing publications suggest vast potential of these materials in such important reactions in electrochemical energy generation as oxidation of alcohols and amines.

References

1. Fan, E.; Li, L.; Wang, Z.; Lin, J.; Huang, Y.; Yao, Y.; Chen, R.; Wu, F. Sustainable Recycling Technology for Li-Ion Batteries and Beyond: Challenges and Future Prospects. *Chem. Rev.* **2020**, *120*, 7020–7063. [CrossRef] [PubMed]
2. Banza Lubaba Nkulu, C.; Casas, L.; Haufroid, V.; De Putter, T.; Saenen, N.D.; Kayembe-Kitenge, T.; Musa Obadia, P.; Kyanika Wa Mukoma, D.; Lunda Ilunga, J.M.; Nawrot, T.S.; et al. Sustainability of artisanal mining of cobalt in DR Congo. *Nat. Sustain.* **2018**, *1*, 495–504. [CrossRef] [PubMed]

3. Poizot, P.; Gaubicher, J.; Renault, S.; Dubois, L.; Liang, Y.; Yao, Y. Opportunities and Challenges for Organic Electrodes in Electrochemical Energy Storage. *Chem. Rev.* **2020**, *120*, 6490–6557. [CrossRef] [PubMed]
4. Xie, Y.; Zhang, K.; Yamauchi, Y.; Oyaizu, K.; Jia, Z. Nitroxide radical polymers for emerging plastic energy storage and organic electronics: Fundamentals, materials, and applications. *Mater. Horiz.* **2021**, *8*, 803–829. [CrossRef] [PubMed]
5. Esser, B.; Dolhem, F.; Becuwe, M.; Poizot, P.; Vlad, A.; Brandell, D. A perspective on organic electrode materials and technologies for next generation batteries. *J. Power Sources* **2021**, *482*, 228814. [CrossRef]
6. Goujon, N.; Casado, N.; Patil, N.; Marcilla, R.; Mecerreyes, D. Organic batteries based on just redox polymers. *Prog. Polym. Sci.* **2021**, *122*, 101449. [CrossRef]
7. Rohland, P.; Schröter, E.; Nolte, O.; Newkome, G.R.; Hager, M.D.; Schubert, U.S. Redox-active polymers: The magic key towards energy storage—A polymer design guideline progress in polymer science. *Prog. Polym. Sci.* **2022**, *125*, 101474. [CrossRef]
8. Tan, Y.; Hsu, S.N.; Tahir, H.; Dou, L.; Savoie, B.M.; Boudouris, B.W. Electronic and Spintronic Open-Shell Macromolecules, Quo Vadis? *J. Am. Chem. Soc.* **2022**, *144*, 626–647. [CrossRef]
9. Hansen, K.A.; Blinco, J.P. Nitroxide radical polymers—A versatile material class for high-tech applications. *Polym. Chem.* **2018**, *9*, 1479–1516. [CrossRef]
10. Muench, S.; Wild, A.; Friebe, C.; Haupler, B.; Janoschka, T.; Schubert, U.S. Polymer-Based Organic Batteries. *Chem. Rev.* **2016**, *116*, 9438–9484. [CrossRef]
11. Janoschka, T.; Hager, M.D.; Schubert, U.S. Powering up the Future: Radical Polymers for Battery Applications. *Adv. Mater.* **2012**, *24*, 6397–6409. [CrossRef] [PubMed]
12. Chen, Y.; Zhuo, S.; Li, Z.; Wang, C. Redox polymers for rechargeable metal-ion batteries. *EnergyChem* **2020**, *2*, 100030. [CrossRef]
13. Kim, K.; Baldaguez Medina, P.; Elbert, J.; Kayiwa, E.; Cusick, R.D.; Men, Y.; Su, X. Molecular Tuning of Redox-Copolymers for Selective Electrochemical Remediation. *Adv. Funct. Mater.* **2020**, *30*, 2004635. [CrossRef]
14. Mohebbati, N.; Prudlik, A.; Scherkus, A.; Gudkova, A.; Francke, R. TEMPO-Modified Polymethacrylates as Mediators in Electrosynthesis—Redox Behavior and Electrocatalytic Activity toward Alcohol Substrates. *ChemElectroChem* **2021**, *8*, 3837–3843. [CrossRef]
15. Yang, S.G.; Park, H.J.; Kim, J.W.; Jung, J.M.; Kim, M.J.; Jegal, H.G.; Kim, I.S.; Kang, M.J.; Wee, G.; Yang, H.Y.; et al. Mito-TEMPO improves development competence by reducing superoxide in preimplantation porcine embryos. *Sci. Rep.* **2018**, *8*, 10130. [CrossRef] [PubMed]
16. Shetty, S.; Kumar, R.; Bharati, S. Mito-TEMPO, a mitochondria-targeted antioxidant, prevents *N*-nitrosodiethylamine-induced hepatocarcinogenesis in mice. *Free Radic. Biol. Med.* **2019**, *136*, 76–86. [CrossRef]
17. Komaba, S.; Tanaka, T.; Ozeki, T.; Taki, T.; Watanabe, H.; Tachikawa, H. Fast redox of composite electrode of nitroxide radical polymer and carbon with polyacrylate binder. *J. Power Sources* **2010**, *195*, 6212–6217. [CrossRef]
18. Bugnon, L.; Morton, C.J.H.; Novak, P.; Vetter, J.; Nesvadba, P. Synthesis of Poly(4-methacryloyloxy-TEMPO) via Group-Transfer Polymerization and Its Evaluation in Organic Radical Battery. *Chem. Mater.* **2007**, *19*, 2910–2914. [CrossRef]
19. Koshika, K.; Chikushi, N.; Sano, N.; Oyaizu, K.; Nishide, H. A TEMPO-substituted polyacrylamide as a new cathode material: An organic rechargeable device composed of polymer electrodes and aqueous electrolyte. *Green Chem.* **2010**, *12*, 1573–1575. [CrossRef]
20. Suguro, M.; Iwasa, S.; Kusachi, Y.; Morioka, Y.; Nakahara, K. Cationic Polymerization of Poly(vinyl ether) Bearing a TEMPO Radical: A New Cathode-Active Material for Organic Radical Batteries. *Macromol. Rapid Commun.* **2007**, *28*, 1929–1933. [CrossRef]
21. Sertkol, S.B.; Sinirlioglu, D.; Esat, B.; Muftuoglu, A.E. A novel cathode material based on polystyrene with pendant TEMPO moieties obtained via click reaction and its use in rechargeable batteries. *J. Polym. Res.* **2015**, *22*, 136. [CrossRef]
22. Nakahara, K.; Iriyama, J.; Iwasa, S.; Suguro, M.; Satoh, M.; Cairns, E.J. Cell properties for modified PTMA cathodes of organic radical batteries. *J. Power Sources* **2007**, *165*, 398–402. [CrossRef]
23. Aqil, M.; Ouhib, F.; Aqil, A.; El Idrissi, A.; Detrembleur, C.; Jérôme, C. Polymer ionic liquid bearing radicals as an active material for organic batteries with ultrafast charge-discharge rate. *Eur. Polym. J.* **2018**, *106*, 242–248. [CrossRef]
24. Suga, T.; Yoshimura, K.; Nishide, H. Nitroxide-Substituted Polyether as a New Material for Batteries. *Macromol. Symp.* **2006**, *245–246*, 416–422. [CrossRef]
25. Qu, J.; Katsumata, T.; Satoh, M.; Wada, J.; Masuda, T. Poly(7-oxanorbornenes) carrying 2,2,6,6-tetramethylpiperidine-1-oxy (TEMPO) radicals: Synthesis and charge/discharge properties. *Polymer* **2009**, *50*, 391–396. [CrossRef]
26. Ibe, T.; Frings, R.B.; Lachowicz, A.; Kyo, S.; Nishide, H. Nitroxide polymer networks formed by Michael addition: On site-cured electrode-active organic coating. *Chem. Commun.* **2010**, *46*, 3475–3477. [CrossRef]
27. Sukegawa, T.; Sato, K.; Oyaizu, K.; Nishide, H. Efficient charge transport of a radical polyether/SWCNT composite electrode for an organic radical battery with high charge-storage density. *RSC Adv.* **2015**, *5*, 15448–15452. [CrossRef]
28. Sukegawa, T.; Masuko, I.; Oyaizu, K.; Nishide, H. Expanding the Dimensionality of Polymers Populated with Organic Robust Radicals toward Flow Cell Application: Synthesis of TEMPO-Crowded Bottlebrush Polymers Using Anionic Polymerization and ROMP. *Macromolecules* **2014**, *47*, 8611–8617. [CrossRef]
29. Zhu, J.; Zhu, T.; Tuo, H.; Zhang, W. Synthesis of a TEMPO-Substituted Polyacrylamide Bearing a Sulfonate Sodium Pendant and Its Properties in an Organic Radical Battery. *Polymers* **2019**, *11*, 2076. [CrossRef]
30. Hickey, D.P.; Milton, R.D.; Chen, D.; Sigman, M.S.; Minteer, S.D. TEMPO-Modified Linear Poly(ethylenimine) for Immobilization-Enhanced Electrocatalytic Oxidation of Alcohols. *ACS Catal.* **2015**, *5*, 5519–5524. [CrossRef]

31. Chen, Y.; Zhang, Y.; Liu, X.; Fan, X.; Bai, B.; Yang, K.; Liang, Z.; Zhang, Z.; Mai, K. Long-Life and High-Power Binder-Free Cathode Based on One-Step Synthesis of Radical Polymers with Multi-Pendant Groups. *Macromol. Rapid Commun.* **2018**, *39*, 1800195. [CrossRef] [PubMed]

32. Qu, J.; Khan, F.Z.; Satoh, M.; Wada, J.; Hayashi, H.; Mizoguchi, K.; Masuda, T. Synthesis and charge/discharge properties of cellulose derivatives carrying free radicals. *Polymer* **2008**, *49*, 1490–1496. [CrossRef]

33. Aydın, M.; Esat, B.; Kılıç, Ç.; Köse, M.E.; Ata, A.; Yılmaz, F. A polythiophene derivative bearing TEMPO as a cathode material for rechargeable batteries. *Eur. Polym. J.* **2011**, *47*, 2283–2294. [CrossRef]

34. Xu, L.; Ji, L.; Wang, G.; Zhang, C.; Su, C. A novel nitroxide radical polymer-containing conductive polyaniline as molecular skeleton: Its synthesis and electrochemical properties as organic cathode. *Ionics* **2016**, *22*, 1377–1385. [CrossRef]

35. Zhang, Y.; Park, A.M.; McMillan, S.R.; Harmon, N.J.; Flatté, M.E.; Fuchs, G.D.; Ober, C.K. Charge Transport in Conjugated Polymers with Pendent Stable Radical Groups. *Chem. Mater.* **2018**, *30*, 4799–4807. [CrossRef]

36. Qu, J.; Fujii, T.; Katsumata, T.; Suzuki, Y.; Shiotsuki, M.; Sanda, F.; Satoh, M.; Wada, J.; Masuda, T. Helical polyacetylenes carrying 2,2,6,6-tetramethyl-1-piperidinyloxy and 2,2,5,5-tetramethyl-1-pyrrolidinyloxy moieties: Their synthesis, properties, and function. *J. Polym. Sci. Part A Polym. Chem.* **2007**, *45*, 5431–5445. [CrossRef]

37. Xu, L.; Yang, F.; Su, C.; Ji, L.; Zhang, C. Synthesis and properties of novel TEMPO-contained polypyrrole derivatives as the cathode material of organic radical battery. *Electrochim. Acta* **2014**, *130*, 148–155. [CrossRef]

38. Yi, J.; Tang, D.; Song, D.; Wu, X.; Shen, Z.; Li, M. Selective oxidation of benzyl alcohol on poly(4-(3-(pyrrol-1-yl)propionamido)-2,2,6,6-tetramethylpiperidin-1-yloxy) electrode. *J. Solid State Electrochem.* **2015**, *19*, 2291–2297. [CrossRef]

39. Li, F.; Gore, D.N.; Wang, S.; Lutkenhaus, J.L. Unusual Internal Electron Transfer in Conjugated Radical Polymers. *Angew. Chem.* **2017**, *56*, 9856–9859. [CrossRef]

40. Schwartz, P.O.; Pejic, M.; Wachtler, M.; Bäuerle, P. Synthesis and characterization of electroactive PEDOT-TEMPO polymers as potential cathode materials in rechargeable batteries. *Synth. Met.* **2018**, *243*, 51–57. [CrossRef]

41. Su, C.; Yang, F.; Xu, L.; Zhu, X.; He, H.; Zhang, C. Radical Polymer Containing a Polytriphenylamine Backbone: Its Synthesis and Electrochemical Performance as the Cathode of Lithium-Ion Batteries. *Chempluschem* **2015**, *80*, 606–611. [CrossRef] [PubMed]

42. Vereshchagin, A.A.; Lukyanov, D.A.; Kulikov, I.R.; Panjwani, N.A.; Alekseeva, E.A.; Behrends, J.; Levin, O.V. The Fast and the Capacious: A [Ni(Salen)]-TEMPO Redox-Conducting Polymer for Organic Batteries. *Batter. Supercaps* **2021**, *4*, 336–346. [CrossRef]

43. Nakahara, K.; Iwasa, S.; Satoh, M.; Morioka, Y.; Iriyama, J.; Suguro, M.; Hasegawa, E. Rechargeable batteries with organic radical cathodes. *Chem. Phys. Lett.* **2002**, *359*, 351–354. [CrossRef]

44. Nevers, D.R.; Brushett, F.R.; Wheeler, D.R. Engineering radical polymer electrodes for electrochemical energy storage. *J. Power Sources* **2017**, *352*, 226–244. [CrossRef]

45. Takahashi, K.; Korolev, K.; Tsuji, K.; Oyaizu, K.; Nishide, H.; Bryuzgin, E.; Navrotskiy, A.; Novakov, I. Facile grafting-onto-preparation of block copolymers of TEMPO and glycidyl methacrylates on an oxide substrate as an electrode-active layer. *Polymer* **2015**, *68*, 310–314. [CrossRef]

46. Koshika, K.; Sano, N.; Oyaizu, K.; Nishide, H. An ultrafast chargeable polymer electrode based on the combination of nitroxide radical and aqueous electrolyte. *Chem. Commun.* **2009**, *7*, 836–838. [CrossRef]

47. Nishide, H.; Suga, T. Organic Radical Battery. *Electrochem. Soc. Interface* **2005**, *14*, 32–36. [CrossRef]

48. Wang, S.; Easley, A.D.; Thakur, R.M.; Ma, T.; Yun, J.; Zhang, Y.; Ober, C.K.; Lutkenhaus, J.L. Quantifying internal charge transfer and mixed ion-electron transfer in conjugated radical polymers. *Chem. Sci.* **2020**, *11*, 9962–9970. [CrossRef]

49. Kemper, T.W.; Larsen, R.E.; Gennett, T. Relationship between Molecular Structure and Electron Transfer in a Polymeric Nitroxyl-Radical Energy Storage Material. *J. Phys. Chem. C* **2014**, *118*, 17213–17220. [CrossRef]

50. Oyaizu, K.; Ando, Y.; Konishi, H.; Nishide, H. Nernstian Adsorbate-like Bulk Layer of Organic Radical Polymers for High-Density Charge Storage Purposes. *J. Am. Chem. Soc.* **2008**, *130*, 14459–14461. [CrossRef]

51. Suga, T.; Pu, Y.J.; Oyaizu, K.; Nishide, H. Electron-Transfer Kinetics of Nitroxide Radicals as an Electrode-Active Material. *Bull. Chem. Soc. Jpn.* **2004**, *77*, 2203–2204. [CrossRef]

52. Nakahara, K.; Oyaizu, K.; Nishide, H. Organic Radical Battery Approaching Practical Use. *Chem. Lett.* **2011**, *40*, 222–227. [CrossRef]

53. Chatgilialoglu, C.; Studer, A. *Encyclopedia of Radicals in Chemistry, Biology, and Materials*; John Wiley & Sons Ltd.: Hoboken, NJ, USA, 2012; Volume 2.

54. Grampp, G.; Rasmussen, K. Solvent dynamical effects on the electron self-exchange rate of the TEMPO/TEMPO+ couple (TEMPO = 2,2,6,6-tetramethyl-1-piperidinyloxy radical) Part I. ESR-linebroadening measurements at T = 298 K. *Phys. Chem. Chem. Phys.* **2002**, *4*, 5546–5549. [CrossRef]

55. Martin, H.J.; Hughes, B.K.; Braunecker, W.A.; Gennett, T.; Dadmun, M.D. The impact of radical loading and oxidation on the conformation of organic radical polymers by small angle neutron scattering. *J. Mater. Chem. A* **2018**, *6*, 15659–15667. [CrossRef]

56. Katsumata, T.; Satoh, M.; Wada, J.; Shiotsuki, M.; Sanda, F.; Masuda, T. Polyacetylene and Polynorbornene Derivatives Carrying TEMPO. Synthesis and Properties as Organic Radical Battery Materials. *Macromol. Rapid Commun.* **2006**, *27*, 1206–1211. [CrossRef]

57. Lutkenhaus, J. A radical advance for conducting polymers. *Science* **2018**, *359*, 1334–1335. [CrossRef]

58. Joo, Y.; Agarkar, V.; Sung, S.H.; Savoie, B.M.; Boudouris, B.W. A nonconjugated radical polymer glass with high electrical conductivity. *Science* **2018**, *359*, 1391–1395. [CrossRef]

59. Oka, K.; Nishide, H. Chapter 4 Radical Polymers for Rechargeable Batteries. In *Redox Polymers for Energy and Nanomedicine*; The Royal Society of Chemistry: London, UK, 2021; pp. 137–165.

60. Tokue, H.; Oyaizu, K.; Sukegawa, T.; Nishide, H. TEMPO/Viologen Electrochemical Heterojunction for Diffusion-Controlled Redox Mediation: A Highly Rectifying Bilayer-Sandwiched Device Based on Cross-Reaction at the Interface between Dissimilar Redox Polymers. *ACS Appl. Mater. Interfaces* **2014**, *6*, 4043–4049. [CrossRef]

61. Suga, T.; Konishi, H.; Nishide, H. Photocrosslinked nitroxide polymer cathode-active materials for application in an organic-based paper battery. *Chem. Commun.* **2007**, *17*, 1730–1732. [CrossRef]

62. Ou, Y.; Zhang, Y.; Xiong, Y.; Hu, Z.; Dong, L. Three-dimensional porous radical polymer/reduced graphene oxide composite with two-electron redox reactions as high-performance cathode for lithium-ion batteries. *Eur. Polym. J.* **2021**, *143*, 110191. [CrossRef]

63. Stolze, C.; Janoschka, T.; Flauder, S.; Müller, F.A.; Hager, M.D.; Schubert, U.S. Investigation of Ice-Templated Porous Electrodes for Application in Organic Batteries. *ACS Appl. Mater. Interfaces* **2016**, *8*, 23614–23623. [CrossRef] [PubMed]

64. Xie, J.; Gu, P.; Zhang, Q. Nanostructured Conjugated Polymers: Toward High-Performance Organic Electrodes for Rechargeable Batteries. *ACS Energy Lett.* **2017**, *2*, 1985–1996. [CrossRef]

65. Nakahara, K.; Oyaizu, K.; Nishide, H. Electrolyte anion-assisted charge transportation in poly(oxoammonium cation/nitroxyl radical) redox gels. *J. Mater. Chem.* **2012**, *22*, 13669–13673. [CrossRef]

66. Chae, I.S.; Koyano, M.; Oyaizu, K.; Nishide, H. Self-doping inspired zwitterionic pendant design of radical polymers toward a rocking-chair-type organic cathode-active material. *J. Mater. Chem. A* **2013**, *1*, 1326–1333. [CrossRef]

67. Tokue, H.; Murata, T.; Agatsuma, H.; Nishide, H.; Oyaizu, K. Charge–Discharge with Rocking-Chair-Type Li+ Migration Characteristics in a Zwitterionic Radical Copolymer Composed of TEMPO and Trifluoromethanesulfonylimide with Carbonate Electrolytes for a High-Rate Li-Ion Battery. *Macromolecules* **2017**, *50*, 1950–1958. [CrossRef]

68. Suga, T.; Sakata, M.; Aoki, K.; Nishide, H. Synthesis of Pendant Radical- and Ion-Containing Block Copolymers via Ring-Opening Metathesis Polymerization for Organic Resistive Memory. *ACS Macro Lett.* **2014**, *3*, 703–707. [CrossRef]

69. Wang, S.; Li, F.; Easley, A.D.; Lutkenhaus, J.L. Real-time insight into the doping mechanism of redox-active organic radical polymers. *Nat. Mater.* **2019**, *18*, 69–75. [CrossRef]

70. Koshika, K.; Sano, N.; Oyaizu, K.; Nishide, H. An Aqueous, Electrolyte-Type, Rechargeable Device Utilizing a Hydrophilic Radical Polymer-Cathode. *Macromol. Chem. Phys.* **2009**, *210*, 1989–1995. [CrossRef]

71. Isogai, A.; Saito, T.; Fukuzumi, H. TEMPO-oxidized cellulose nanofibers. *Nanoscale* **2011**, *3*, 71–85. [CrossRef]

72. Li, F.; Zhang, Y.; Kwon, S.R.; Lutkenhaus, J.L. Electropolymerized Polythiophenes Bearing Pendant Nitroxide Radicals. *ACS Macro Lett.* **2016**, *5*, 337–341. [CrossRef]

73. Xie, Y.; Zhang, K.; Monteiro, M.J.; Jia, Z. Conjugated Nitroxide Radical Polymers: Synthesis and Application in Flexible Energy Storage Devices. *ACS Appl. Mater. Interfaces* **2019**, *11*, 7096–7103. [CrossRef] [PubMed]

74. Liu, K.; Perera, K.; Wang, Z.; Mei, J.; Boudouris, B.W. Impact of open-shell loading on mass transport and doping in conjugated radical polymers. *J. Polym. Sci.* **2021**, *59*, 2771–2782. [CrossRef]

75. Li, F.; Wang, S.; Zhang, Y.; Lutkenhaus, J.L. Electrochemical Energy Storage in Poly(dithieno[3,2-b:2′,3′-d]pyrrole) Bearing Pendant Nitroxide Radicals. *Chem. Mater.* **2018**, *30*, 5169–5174. [CrossRef]

76. Suguro, M.; Iwasa, S.; Nakahara, K. Fabrication of a Practical and Polymer-Rich Organic Radical Polymer Electrode and Its Rate Dependence. *Macromol. Rapid Commun.* **2008**, *29*, 1635–1639. [CrossRef]

77. Suguro, M.; Iwasa, S.; Nakahara, K. Effect of Ethylene Oxide Structures in TEMPO Polymers on High Rate Discharge Properties. *Electrochem. Solid-State Lett.* **2009**, *12*, A194. [CrossRef]

78. Hergué, N.; Ernould, B.; Minoia, A.; Lazzaroni, R.; Gohy, J.F.; Dubois, P.; Coulembier, O. Improving the Performance of Batteries by Using Multi-Pyrene PTMA Structures. *Batter. Supercaps* **2018**, *1*, 102–109. [CrossRef]

79. Chae, I.S.; Koyano, M.; Sukegawa, T.; Oyaizu, K.; Nishide, H. Redox equilibrium of a zwitterionic radical polymer in a non-aqueous electrolyte as a novel Li+ host material in a Li-ion battery. *J. Mater. Chem. A* **2013**, *1*, 9608–9611. [CrossRef]

80. Qin, H.; Liu, X.; Huang, J.; Liang, H.; Zhang, Z.; Lu, J. Design and Synthesis of a Facile Solution-Processing and Ultrastable Crosslinkable Branched Nitroxide Polymer. *Macromol. Chem. Phys.* **2019**, *220*, 1900068. [CrossRef]

81. Zhang, X.; Li, H.; Li, L.; Lu, G.; Zhang, S.; Gu, L.; Xia, Y.; Huang, X. Polyallene with pendant nitroxyl radicals. *Polymer* **2008**, *49*, 3393–3398. [CrossRef]

82. Hatakeyama-Sato, K.; Wakamatsu, H.; Matsumoto, S.; Sadakuni, K.; Matsuoka, K.; Nagatsuka, T.; Oyaizu, K. TEMPO-Substituted Poly(ethylene sulfide) for Solid-State Electro-Chemical Charge Storage. *Macromol. Rapid Commun.* **2021**, *42*, 2000607. [CrossRef]

83. Zhang, K.; Xie, Y.; Monteiro, M.J.; Jia, Z. Triazole-enabled small TEMPO cathodes for lithium-organic batteries. *Energy Storage Mater.* **2021**, *35*, 122–129. [CrossRef]

84. Aqil, M.; Aqil, A.; Ouhib, F.; El Idrissi, A.; Dahbi, M.; Detrembleur, C.; Jérôme, C. Nitroxide TEMPO-containing PILs: Kinetics study and electrochemical characterizations. *Eur. Polym. J.* **2021**, *152*, 110453. [CrossRef]

85. Lee, S.H.; Kim, J.K.; Cheruvally, G.; Choi, J.W.; Ahn, J.H.; Chauhan, G.S.; Song, C.E. Electrochemical properties of new organic radical materials for lithium secondary batteries. *J. Power Sources* **2008**, *184*, 503–507. [CrossRef]

86. Kim, K.; Kim, J.K. Organic di-radical rechargeable battery with an ionic liquid-based gel polymer electrolyte. *Korean J. Chem. Eng.* **2016**, *33*, 858–861. [CrossRef]

87. Suguro, M.; Mori, A.; Iwasa, S.; Nakahara, K.; Nakano, K. Syntheses and Electrochemical Properties of TEMPO Radical Substituted Silicones: Active Material for Organic Radical Batteries. *Macromol. Chem. Phys.* **2009**, *210*, 1402–1407. [CrossRef]

88. Lu, C.; Pan, G.; Mao, Z.; Shi, L.; Huang, Q.; Tian, W.; Hu, Y.; Wu, H.; Wang, Z.; Sun, K. Multiradical-stabilized hollow carbon spheres as a pressure-resistant cathode for fast lithium/sodium storage with excellent performance. *J. Mater. Chem. A* **2020**, *8*, 8875–8882. [CrossRef]

89. Gopinath, A.; Sultan Nasar, A. Electroactive six arm star poly(2,2,6,6-tetramethylpiperidinyloxy methacrylate): Synthesis and application as cathode material for rechargeable Li-ion batteries. *Polymer* **2019**, *178*, 121601. [CrossRef]

90. Aydin, M.; Gorur, M.; Yilmaz, F. Phosphazene-cored star polymer bearing redox-active side groups as a cathode-active material in Li-ion batteries. *React. Funct. Polym.* **2016**, *102*, 11–19. [CrossRef]

91. Lin, H.C.; Li, C.C.; Lee, J.T. Nitroxide polymer brushes grafted onto silica nanoparticles as cathodes for organic radical batteries. *J. Power Sources* **2011**, *196*, 8098–8103. [CrossRef]

92. Wang, Y.H.; Hung, M.K.; Lin, C.H.; Lin, H.C.; Lee, J.T. Patterned nitroxide polymer brushes for thin-film cathodes in organic radical batteries. *Chem. Commun.* **2011**, *47*, 1249–1251. [CrossRef]

93. Hung, M.K.; Wang, Y.H.; Lin, C.H.; Lin, H.C.; Lee, J.T. Synthesis and electrochemical behaviour of nitroxidepolymer brush thin-film electrodes for organic radical batteries. *J. Mater. Chem.* **2012**, *22*, 1570–1577. [CrossRef]

94. Liu, C.M.; Chen, J.; Wang, F.Q.; Yi, B.L. Improvement of electrochemical properties of PTMA cathode by using carbon blacks with high specific surface area. *Russ. J. Electrochem.* **2012**, *48*, 1052–1057. [CrossRef]

95. Kim, T.S.; Lim, J.E.; Oh, M.S.; Kim, J.K. Carbon conductor- and binder-free organic electrode for flexible organic rechargeable batteries with high energy density. *J. Power Sources* **2017**, *361*, 15–20. [CrossRef]

96. Guo, W.; Yin, Y.X.; Xin, S.; Guo, Y.G.; Wan, L.J. Superior radical polymer cathode material with a two-electron process redox reaction promoted by graphene. *Energy Environ. Sci.* **2012**, *5*, 5221–5225. [CrossRef]

97. Ernould, B.; Devos, M.; Bourgeois, J.P.; Rolland, J.; Vlad, A.; Gohy, J.F. Grafting of a redox polymer onto carbon nanotubes for high capacity battery materials. *J. Mater. Chem. A* **2015**, *3*, 8832–8839. [CrossRef]

98. Ernould, B.; Bertrand, O.; Minoia, A.; Lazzaroni, R.; Vlad, A.; Gohy, J.F. Electroactive polymer/carbon nanotube hybrid materials for energy storage synthesized via a "grafting to" approach. *RSC Adv.* **2017**, *7*, 17301–17310. [CrossRef]

99. Lin, C.H.; Lee, J.T.; Yang, D.R.; Chen, H.W.; Wu, S.T. Nitroxide radical polymer/carbon-nanotube-array electrodes with improved C-rate performance in organic radical batteries. *RSC Adv.* **2015**, *5*, 33044–33048. [CrossRef]

100. Vlad, A.; Rolland, J.; Hauffman, G.; Ernould, B.; Gohy, J.F. Melt-Polymerization of TEMPO Methacrylates with Nano Carbons Enables Superior Battery Materials. *ChemSusChem* **2015**, *8*, 1692–1696. [CrossRef]

101. Hauffman, G.; Maguin, Q.; Bourgeois, J.P.; Vlad, A.; Gohy, J.F. Micellar Cathodes from Self-Assembled Nitroxide-Containing Block Copolymers in Battery Electrolytes. *Macromol. Rapid Commun.* **2014**, *35*, 228–233. [CrossRef]

102. Kim, J.K. Micro-fibrous organic radical electrode to improve the electrochemical properties of organic rechargeable batteries. *J. Power Sources* **2013**, *242*, 683–686. [CrossRef]

103. Kim, J.K.; Cheruvally, G.; Choi, J.W.; Ahn, J.H.; Lee, S.H.; Choi, D.S.; Song, C.E. Effect of radical polymer cathode thickness on the electrochemical performance of organic radical battery. *Solid State Ion.* **2007**, *178*, 1546–1551. [CrossRef]

104. Kim, J.K.; Cheruvally, G.; Ahn, J.H.; Seo, Y.G.; Choi, D.S.; Lee, S.H.; Song, C.E. Organic radical battery with PTMA cathode: Effect of PTMA content on electrochemical properties. *J. Ind. Eng. Chem.* **2008**, *14*, 371–376. [CrossRef]

105. Kim, Y.; Jo, C.; Lee, J.; Lee, C.W.; Yoon, S. An ordered nanocomposite of organic radical polymer and mesocellular carbon foam as cathode material in lithium ion batteries. *J. Mater. Chem.* **2012**, *22*, 1453–1458. [CrossRef]

106. Kim, J.K.; Scheers, J.; Ahn, J.H.; Johansson, P.; Matic, A.; Jacobsson, P. Nano-fibrous polymer films for organic rechargeable batteries. *J. Mater. Chem. A* **2013**, *1*, 2426–2430. [CrossRef]

107. Zhang, K.; Hu, Y.; Wang, L.; Fan, J.; Monteiro, M.J.; Jia, Z. The impact of the molecular weight on the electrochemical properties of poly(TEMPO methacrylate). *Polym. Chem.* **2017**, *8*, 1815–1823. [CrossRef]

108. Kim, J.K.; Cheruvally, G.; Choi, J.W.; Ahn, J.H.; Choi, D.S.; Song, C.E. Rechargeable Organic Radical Battery with Electrospun, Fibrous Membrane-Based Polymer Electrolyte. *J. Electrochem. Soc.* **2007**, *154*, A839. [CrossRef]

109. Nishide, H.; Iwasa, S.; Pu, Y.J.; Suga, T.; Nakahara, K.; Satoh, M. Organic radical battery: Nitroxide polymers as a cathode-active material. *Electrochim. Acta* **2004**, *50*, 827–831. [CrossRef]

110. Nakahara, K.; Iriyama, J.; Iwasa, S.; Suguro, M.; Satoh, M.; Cairns, E.J. Al-laminated film packaged organic radical battery for high-power applications. *J. Power Sources* **2007**, *163*, 1110–1113. [CrossRef]

111. Muench, S.; Gerlach, P.; Burges, R.; Strumpf, M.; Hoeppener, S.; Wild, A.; Lex-Balducci, A.; Balducci, A.; Brendel, J.C.; Schubert, U.S. Emulsion Polymerizations for a Sustainable Preparation of Efficient TEMPO-Based Electrodes. *ChemSusChem* **2021**, *14*, 449–455. [CrossRef]

112. Deng, L.F.; Li, X.H.; Xiao, L.X.; Zhang, Y.H. Synthesis and electrochemical properties of polyradical cathode material for lithium second batteries. *J. Cent. South Univ. Technol.* **2003**, *10*, 190–194. [CrossRef]

113. Kim, J.K.; Ahn, J.H.; Cheruvally, G.; Chauhan, G.S.; Choi, J.W.; Kim, D.S.; Ahn, H.J.; Lee, S.H.; Song, C.E. Electrochemical properties of rechargeable organic radical battery with PTMA cathode. *Met. Mater. Int.* **2009**, *15*, 77–82. [CrossRef]

114. Zhang, K.; Hu, Y.; Wang, L.; Monteiro, M.J.; Jia, Z. Pyrene-Functionalized PTMA by NRC for Greater π–π Stacking with rGO and Enhanced Electrochemical Properties. *ACS Appl. Mater. Interfaces* **2017**, *9*, 34900–34908. [CrossRef] [PubMed]

115. Vereshchagin, A.A.; Vlasov, P.S.; Konev, A.S.; Yang, P.; Grechishnikova, G.A.; Levin, O.V. Novel highly conductive cathode material based on stable-radical organic framework and polymerized nickel complex for electrochemical energy storage devices. *Electrochim. Acta* **2019**, *295*, 1075–1084. [CrossRef]

116. Iwasa, S.; Nishi, T.; Sato, H.; Nakamura, S. Flexibility and High-Rate Discharge Properties of Organic Radical Batteries with Gel-State Electrodes. *J. Electrochem. Soc.* **2017**, *164*, A884–A888. [CrossRef]

117. Wang, S.; Park, A.M.G.; Flouda, P.; Easley, A.D.; Li, F.; Ma, T.; Fuchs, G.D.; Lutkenhaus, J.L. Solution-Processable Thermally Crosslinked Organic Radical Polymer Battery Cathodes. *ChemSusChem* **2020**, *13*, 2371–2378. [CrossRef]

118. Sato, K.; Sukegawa, T.; Oyaizu, K.; Nishide, H. Synthesis of Poly(TEMPO-Substituted Glycidyl Ether) by Utilizing t-BuOK/18-Crown-6 for an Organic Cathode-Active Material. *Macromol. Symp.* **2015**, *351*, 90–96. [CrossRef]

119. Oyaizu, K.; Suga, T.; Yoshimura, K.; Nishide, H. Synthesis and Characterization of Radical-Bearing Polyethers as an Electrode-Active Material for Organic Secondary Batteries. *Macromolecules* **2008**, *41*, 6646–6652. [CrossRef]

120. Hatakeyama-Sato, K.; Wakamatsu, H.; Yamagishi, K.; Fujie, T.; Takeoka, S.; Oyaizu, K.; Nishide, H. Ultrathin and Stretchable Rechargeable Devices with Organic Polymer Nanosheets Conformable to Skin Surface. *Small* **2019**, *15*, 1805296. [CrossRef]

121. Chikushi, N.; Yamada, H.; Oyaizu, K.; Nishide, H. TEMPO-substituted polyacrylamide for an aqueous electrolyte-typed and organic-based rechargeable device. *Sci. China Chem.* **2012**, *55*, 822–829. [CrossRef]

122. Suga, T.; Ohshiro, H.; Sugita, S.; Oyaizu, K.; Nishide, H. Emerging *N*-Type Redox-Active Radical Polymer for a Totally Organic Polymer-Based Rechargeable Battery. *Adv. Mater.* **2009**, *21*, 1627–1630. [CrossRef]

123. Katsumata, T.; Qu, J.; Shiotsuki, M.; Satoh, M.; Wada, J.; Igarashi, J.; Mizoguchi, K.; Masuda, T. Synthesis, Characterization, and Charge/Discharge Properties of Polynorbornenes Carrying 2,2,6,6-Tetramethylpiperidine-1-oxy Radicals at High Density. *Macromolecules* **2008**, *41*, 1175–1183. [CrossRef]

124. Dai, Y.; Zhang, Y.; Gao, L.; Xu, G.; Xie, J. Electrochemical Performance of Organic Radical Cathode with Ionic Liquid Based Electrolyte. *J. Electrochem. Soc.* **2011**, *158*, A291. [CrossRef]

125. Qu, J.; Morita, R.; Satoh, M.; Wada, J.; Terakura, F.; Mizoguchi, K.; Ogata, N.; Masuda, T. Synthesis and Properties of DNA Complexes Containing 2,2,6,6-Tetramethyl-1-piperidinoxy (TEMPO) Moieties as Organic Radical Battery Materials. *Chem.–A Eur. J.* **2008**, *14*, 3250–3259. [CrossRef] [PubMed]

126. Lebègue, E.; Brousse, T.; Gaubicher, J.; Retoux, R.; Cougnon, C. Toward fully organic rechargeable charge storage devices based on carbon electrodes grafted with redox molecules. *J. Mater. Chem. A* **2014**, *2*, 8599–8602. [CrossRef]

127. Du, Z.; Ai, W.; Xie, L.; Huang, W. Organic radical functionalized graphene as a superior anode material for lithium-ion batteries. *J. Mater. Chem. A* **2014**, *2*, 9164–9168. [CrossRef]

128. Aqil, M.; Dahbi, M.; Saadoune, I.; Idrissi, A.E.; Aqil, A.; Jérôme, C. Functionalized Graphite Nanoplatelet by Nitroxide Radical PILs as Anode Materials for Li-ion Battery. In Proceedings of the 2019 7th International Renewable and Sustainable Energy Conference (IRSEC), Agadir, Morocco, 27–30 November 2019; pp. 1–4.

129. Guo, X.; Facchetti, A. The journey of conducting polymers from discovery to application. *Nat. Mater.* **2020**, *19*, 922–928. [CrossRef]

130. Inzelt, G. *Conducting Polymers a New Era in Electrochemistry*; Springer: Berlin/Heidelberg, Germany; New York, NY, USA, 2012.

131. MacDiarmid, A.G.; Mammone, R.J.; Kaner, R.B.; Porter, L. The concept of 'doping' of conducting polymers: The role of reduction potentials. *Philos. Trans. R. Soc. London. Ser. A Math. Phys. Sci.* **1997**, *314*, 3–15. [CrossRef]

132. Shirakawa, H.; Louis, E.J.; MacDiarmid, A.G.; Chiang, C.K.; Heeger, A.J. Synthesis of electrically conducting organic polymers: Halogen derivatives of polyacetylene, (CH) x. *J. Chem. Soc. Chem. Commun.* **1977**, *16*, 578–580. [CrossRef]

133. Qu, J.; Katsumata, T.; Satoh, M.; Wada, J.; Igarashi, J.; Mizoguchi, K.; Masuda, T. Synthesis and charge/discharge properties of polyacetylenes carrying 2,2,6,6-tetramethyl-1-piperidinoxy radicals. *Chemistry* **2007**, *13*, 7965–7973. [CrossRef]

134. Bahceci, S.; Esat, B. A polyacetylene derivative with pendant TEMPO group as cathode material for rechargeable batteries. *J. Power Sources* **2013**, *242*, 33–40. [CrossRef]

135. Qu, J.; Katsumata, T.; Satoh, M.; Wada, J.; Masuda, T. Synthesis and Properties of Polyacetylene and Polynorbornene Derivatives Carrying 2,2,5,5-Tetramethyl-1-pyrrolidinyloxy Moieties. *Macromolecules* **2007**, *40*, 3136–3144. [CrossRef]

136. Xu, L.; Guo, P.; He, H.; Zhou, N.; Ma, J.; Wang, G.; Zhang, C.; Su, C. Preparation of TEMPO-contained pyrrole copolymer by in situ electrochemical polymerization and its electrochemical performances as cathode of lithium ion batteries. *Ionics* **2017**, *23*, 1375–1382. [CrossRef]

137. Xu, L.H.; Yang, F.; Su, C.; Zhang, C. Research of Properties on Li-Ion Batteries Based on a Polypyrrole Derivative Bearing TEMPO as a Cathode Material. *Adv. Mater. Res.* **2014**, *936*, 447–451. [CrossRef]

138. Oyaizu, K.; Tatsuhira, H.; Nishide, H. Facile charge transport and storage by a TEMPO-populated redox mediating polymer integrated with polyaniline as electrical conducting path. *Polym. J.* **2014**, *47*, 212–219. [CrossRef]

139. Schon, T.B.; McAllister, B.T.; Li, P.F.; Seferos, D.S. The rise of organic electrode materials for energy storage. *Chem. Soc. Rev.* **2016**, *45*, 6345–6404. [CrossRef] [PubMed]

140. Xiong, J.; Wei, Z.; Xu, T.; Zhang, Y.; Xiong, C.; Dong, L. Polytriphenylamine derivative with enhanced electrochemical performance as the organic cathode material for rechargeable batteries. *Polymer* **2017**, *130*, 135–142. [CrossRef]

141. Aydin, M.; Esat, B. A polythiophene derivative bearing two electroactive groups per monomer as a cathode material for rechargeable batteries. *J. Solid State Electrochem.* **2015**, *19*, 2275–2281. [CrossRef]

142. Casado, N.; Hernandez, G.; Veloso, A.; Devaraj, S.; Mecerreyes, D.; Armand, M. PEDOT Radical Polymer with Synergetic Redox and Electrical Properties. *ACS Macro Lett.* **2016**, *5*, 59–64. [CrossRef]

143. Assumma, L.; Kervella, Y.; Mouesca, J.M.; Mendez, M.; Maurel, V.; Dubois, L.; Gutel, T.; Sadki, S. A New Conducting Copolymer Bearing Electro-Active Nitroxide Groups as Organic Electrode Materials for Batteries. *ChemSusChem* **2020**, *13*, 2419–2427. [CrossRef]

144. Hagemann, T.; Winsberg, J.; Grube, M.; Nischang, I.; Janoschka, T.; Martin, N.; Hager, M.D.; Schubert, U.S. An aqueous all-organic redox-flow battery employing a (2,2,6,6-tetramethylpiperidin-1-yl)oxyl-containing polymer as catholyte and dimethyl viologen dichloride as anolyte. *J. Power Sources* **2018**, *378*, 546–554. [CrossRef]

145. Hagemann, T.; Strumpf, M.; Schröter, E.; Stolze, C.; Grube, M.; Nischang, I.; Hager, M.D.; Schubert, U.S. (2,2,6,6-Tetramethylpiperidin-1-yl)oxyl-Containing Zwitterionic Polymer as Catholyte Species for High-Capacity Aqueous Polymer Redox Flow Batteries. *Chem. Mater.* **2019**, *31*, 7987–7999. [CrossRef]

146. Janoschka, T.; Martin, N.; Martin, U.; Friebe, C.; Morgenstern, S.; Hiller, H.; Hager, M.D.; Schubert, U.S. An aqueous, polymer-based redox-flow battery using non-corrosive, safe, and low-cost materials. *Nature* **2015**, *527*, 78–81. [CrossRef] [PubMed]

147. Janoschka, T.; Morgenstern, S.; Hiller, H.; Friebe, C.; Wolkersdörfer, K.; Häupler, B.; Hager, M.D.; Schubert, U.S. Synthesis and characterization of TEMPO- and viologen-polymers for water-based redox-flow batteries. *Polym. Chem.* **2015**, *6*, 7801–7811. [CrossRef]

148. Winsberg, J.; Janoschka, T.; Morgenstern, S.; Hagemann, T.; Muench, S.; Hauffman, G.; Gohy, J.F.; Hager, M.D.; Schubert, U.S. Poly(TEMPO)/Zinc Hybrid-Flow Battery: A Novel, "Green," High Voltage, and Safe Energy Storage System. *Adv. Mater.* **2016**, *28*, 2238–2243. [CrossRef] [PubMed]

149. Kozhunova, E.Y.; Gvozdik, N.A.; Motyakin, M.V.; Vyshivannaya, O.V.; Stevenson, K.J.; Itkis, D.M.; Chertovich, A.V. Redox-Active Aqueous Microgels for Energy Storage Applications. *J. Phys. Chem. Lett.* **2020**, *11*, 10561–10565. [CrossRef] [PubMed]

150. Hatakeyama-Sato, K.; Nagano, T.; Noguchi, S.; Sugai, Y.; Du, J.; Nishide, H.; Oyaizu, K. Hydrophilic Organic Redox-Active Polymer Nanoparticles for Higher Energy Density Flow Batteries. *ACS Appl. Polym. Mater.* **2019**, *1*, 188–196. [CrossRef]

151. Winsberg, J.; Muench, S.; Hagemann, T.; Morgenstern, S.; Janoschka, T.; Billing, M.; Schacher, F.H.; Hauffman, G.; Gohy, J.F.; Hoeppener, S.; et al. Polymer/zinc hybrid-flow battery using block copolymer micelles featuring a TEMPO corona as catholyte. *Polym. Chem.* **2016**, *7*, 1711–1718. [CrossRef]

152. Beejapur, H.A.; Zhang, Q.; Hu, K.; Zhu, L.; Wang, J.; Ye, Z. TEMPO in Chemical Transformations: From Homogeneous to Heterogeneous. *ACS Catal.* **2019**, *9*, 2777–2830. [CrossRef]

153. Schille, B.; Giltzau, N.O.; Francke, R. On the Use of Polyelectrolytes and Polymediators in Organic Electrosynthesis. *Angew. Chem. Int. Ed.* **2018**, *57*, 422–426. [CrossRef]

154. Macazo, F.C.; Hickey, D.P.; Abdellaoui, S.; Sigman, M.S.; Minteer, S.D. Polymer-immobilized, hybrid multi-catalyst architecture for enhanced electrochemical oxidation of glycerol. *Chem. Commun.* **2017**, *53*, 10310–10313. [CrossRef]

155. Franco, J.H.; Neto, S.A.; Hickey, D.P.; Minteer, S.D.; de Andrade, A.R. Hybrid catalyst cascade architecture enhancement for complete ethanol electrochemical oxidation. *Biosens. Bioelectron.* **2018**, *121*, 281–286. [CrossRef] [PubMed]

156. Lu, J.J.; Ma, J.Q.; Yi, J.M.; Shen, Z.L.; Zhong, Y.J.; Ma, C.A.; Li, M.C. Electrochemical Polymerization of Pyrrole Containing TEMPO Side Chain on Pt Electrode and Its Electrochemical Activity. *Electrochim. Acta* **2014**, *130*, 412–417. [CrossRef]

157. Wang, X.; Ma, J.; Song, D.; Shen, Z.; Li, M.; Ma, C. Characterization and Electrocatalytic Activity of Poly(4-thienylacetyl-oxy-2,2,6,6-tetramethylpiperidin-1-yloxy) Prepared by Electrochemical Polymerization. *ECS Electrochem. Lett.* **2014**, *3*, H12–H15. [CrossRef]

158. Niu, P.; Cai, Y.; Guo, M.; Shen, Z.; Li, M. Preparation and electrochemical performance of TEMPO-modified polyterthiophene electrode obtained by electropolymerization. *Electrochem. Commun.* **2020**, *110*, 106623. [CrossRef]

159. Niu, P.; Huang, H.; Zhao, L.; Zhang, C.; Shen, Z.; Li, M. Preparation of poly(carbazole-TEMPO) electrode and its electrochemical performance. *J. Electroanal. Chem.* **2021**, *894*, 115352. [CrossRef]

160. Kashiwagi, Y.; Chiba, S.; Anzai, J.I. Amperometric determination of optically active 1-phenylethanol using chiral nitroxyl radical-modified polypyrrole films prepared by electrochemical polymerization. *J. Electroanal. Chem.* **2004**, *566*, 257–262. [CrossRef]

161. Kashiwagi, Y.; Ono, T.; Tsunoda, M.; Takahashi, S.; Obata, T.; Sone, T. Voltammetric Behavior of Mediator-Modified Electrode by Electrochemical Polymerization of Nitroxyl Radical Precursor Containing Pyrrole Side Chain. *Heterocycles* **2010**, *81*, 2771–2780. [CrossRef]

162. Kashiwagi, Y.; Tsunoda, M.; Ono, T. Voltammetric Behavior of Mediator-Modified Electrode by Electrochemical Copolymerization of Nitroxyl Radical Precursor Containing Pyrrole Side Chain and Thiophenes. *Heterocycles* **2011**, *83*, 2517–2524. [CrossRef]

163. Ono, T.; Sato, K.; Shimizu, S.; Yoshida, K.; Dairaku, T.; Suzuki, Y.; Kashiwagi, Y. Electrocatalytic Oxidation of Carbohydrates Mediated by Nitroxyl Radical-modified Electrodes in Aqueous Solution. *Electroanalysis* **2018**, *30*, 24–26. [CrossRef]

164. Place, S.D.; Kavanagh, P. Electroactivity of PIPO nitroxide radical polymer films. *Electrochim. Acta* **2021**, *392*, 139044. [CrossRef]

165. Kashiwagi, Y.; Kurashima, F.; Kikuchi, C.; Anzai, J.I.; Osa, T.; Bobbin, J.M. Electrocatalytic Oxidation of Amines to Nitriles on a TEMPO-modified Graphite Felt Electrode (TEMPO = 2,2,6,6-tetramethylpiperidin-1-yloxyl). *J. Chin. Chem. Soc.* **1998**, *45*, 135–138. [CrossRef]

166. MacCorquodale, F.; Crayston, J.A.; Walton, J.C.; Worsfold, D.J. Synthesis and electrochemical characterisation of poly(tempoacrylate). *Tetrahedron Lett.* **1990**, *31*, 771–774. [CrossRef]

167. Kashiwagi, Y.; Takamori, Y.; Yoshida, K.; Ono, T. Electrocatalytic Oxidation of Amines on a Mediator-Modified Electrode by Electrochemical Copolymerization of Nitroxyl Radical Precursor Containing Pyrrole Side Chain and Bithiophene. *Electroanalysis* **2013**, *25*, 2575–2577. [CrossRef]